Accessing Thermal and Mechanical Performance of 3D-Printed Polymer Structures created with Fused Filament Fabrication

Shirani Dalugama Mudiyanselage

Degree Thesis

Mechanical and Sustainable Engineering

2025

Degree Thesis

Shirani Dalugama Mudiyanselage

Assessing Thermal and Mechanical Performance of 3D-Printed Polymer Structures created by Fused Filament Fabrication

Arcada University of Applied Sciences: Mechanical and Sustainable Engineering, 2021.

Commissioned by:

Arcada University of Applied Science

Abstract:

This study primarily focuses on assessing thermal and mechanical performance of 3D printed polymer honeycomb structures from Hyper PLA material through fused filament fabrication method. Two types of own digital models were designed with SolidWorks software. These two geometries were considered into two directions, perpendicular and longitudinal directions to the honeycomb patterns. They were named as Design 1 – horizontal, Design 2 – vertical, Design 2 – horizontal and Design 2 – vertical. The test specimens for heat transfer tests and mechanical tests (tensile and flexural) were designed separately. The dimensions of the specimen for heat transfer were 39.25*39.25*32 mm^3. According to the standard codes, ISO 527 and ISO 179, test specimens for tensile test and flexural test were designed. Then all test specimens were printed through fused filament fabrication method. The slicing parameters were 100% infill density, 200 mm/min speed, 0.2 mm layer thickness, and rectilinear infill pattern. The printing parameters were 220 °C, bed temperature 53°C and temperature and surrounding temperature 34 °C. The speed of cooling fan was 0-30% initially up to 1-3 layers and after that 100%. Steady-state heat conduction tests were carried out for these four geometries with the known heat source (62.1 V and 0.13 A) for 32mm thick side. The temperatures at heated surface (T1) and cold surface (T2) were around 326.25 K to 298.55K which was used to calculate the thermal conductivity. The results were laid between 6.211 to 7.657 W/K.m for all cases. A computational modelling with COMSOL was carried out to ensure the result obtained from steady-state heat conduction test. COMSOL gave the almost same values of the experiment in horizontal direction. Test specimens in all four configurations for tensile and flexural testing were carried out by universal testing machine under test codes the code ISO 527 and ISO 178 respectively. It revealed that the highest young modulus (1639.80 MPa), yield strength (13.99 MPa) and flexural modulus (2155.38 MPa) are laid with Design 1-Horizontal sample while maximum ultimate tensile strength (32.336 MPa) and flexural strength (65.198 MPa) are Design 2-Horizontal sample.

Keywords:

3D printing, fused filament fabrication, Hyper PLA, thermal performance, mechanical performance, Steady-state heat conduction test, mechanical test, thermal insulation.

Contents

1. Background

Thermal insulation refers to materials or systems used to retain heat by reducing the heat transfer through its boundaries by means of conduction, convection and radiation and plays a vital role in making a comfortable life by indoor air quality. It provides not only a comfort living environment but also energy conservation [1,2] which is vital for environmental sustainability and economic saving. For instance, increasing of energy consumption buildings accounts for a significant share of global energy consumption (over 30% of global final energy demand and 55% of global electricity use) and space heating consuming a substantial portion of them (38% for non-residential and 29% for residential buildings) [3,4]. Insulating walls effectively is crucial to reducing energy demand and improving indoor thermal efficiency. Conventional insulation materials, such as fibreglass and foam, often present challenges including high embodied energy, design limitations, and re-cyclability issues [5,6,7]. Application of thermal insulation is in board area such living buildings, workplaces, fluid flowing through pipes, transportation, aircrafts and space shuttles etc. A high strength/volume ratio insulation material is crucial in reducing the total weight of structures, particularly in aircrafts and space shuttles, and making them more economical [41,42]. Therefore, due to rising energy consumption and global environmental concerns, there is a growing demand for efficient and sustainable thermal insulation materials. Innovation an energy efficient, light weight, high strength and sustainable thermal insulation material is the urgent need because it can minimize the energy loss, enhance the thermal regulation and reduce the overburden to the ecosystem. As one of the most developing technology, additive manufacturing (AM) allows to manufacture a versatile, cost effective, adaptable and eco-friendly advanced thermal insulations.

AM allows for different types of manufacturing process which can be selected based on different types of materials. Material extrusion (Fused Filament Fabrication (FFF)) is for thermoplastic filaments, light polymerized, and material jetting are for photopolymer resins while powder bed, powder fed, binder jetting and wire methods are for powdered materials, etc. [8,9,10]. There is a wide range of filaments which are used in FFF based on natural, synthetic, or recycled polymer materials such as Polylactic Acid (PLA), PETG Polyethylene Terephthalate Glycol-modified (PETG), Thermoplastic Polyurethane, Acrylonitrile Butadiene Styrene (ABS), Polycarbonate (PC), Polypropylene (PP), High Impact Polystyrene (HIPS), Nylon, Metals, Alloys, wood, linen, & other materials [11,12,13]. Some filament materials are biodegradable (PLA) and mechanical degradation is needed for some of them and there is no solid waste. FFF is considered as one of the fastest methods for printing small and large objects, and it is also low budget [14]. The process is heated filament material, is extruded through a nozzle, layer by layer on heated bed, to create an object. The quality of the products depends on several parameters such as printing speed, layer thickness, print orientation, raster angle, infill pattern, fill density, nozzle temperature, extrusion temperature, etc. [15,16,17]. The various infill patterns are available, and they are mostly unique for printer software. The slicing software which will be used for fabricated samples is “UltiMaker Cura”, the inbuilt infill 2 patterns are grid, lines, triangles, tri-hexagon, cubic, cubic subdivision, octet, quarter cubic, concentric, zig-zag, cross, cross 3D, gyroid, lightning [18] and it is allowed to make custom infill patterns such as honeycomb or other desired designs [19]. A review study [20] gives a broad discussion on 3D printing technology, methods, materials, developments, industrial applications and challengers. Testing of the 3D printed materials is an essential task in quality control and assurance. The frequently carry

out tests are uniaxial tension test, 3-point bend flexure test and compression test in laboratory and field [21]. Additive manufacturing allows to create more flexible, budget solution for industry, it has own challengers [22, 23] and industries should be considered about them.

1.1 Aim of Study

Investigating the thermal and mechanical performance of 3D printed polymer structures which were fabricated through FFF with different orientations to assess the suitability in thermal insulation applications is the aim of this thesis. By analysing how material properties, structural design and process parameters influence the performance of 3D printed structures as thermal insulation, this study aims to identify the optimal configurations for high efficiency lightweight insulation

1.2 Research objective

The objective of this study is to bridge the gap by conducting a systematic assessment of the thermal and mechanical performance of 3D-printed polymer structures created using FFF.

1. Designing the digital models to print using Fused filament fabrication with different configurations.
2. Designing of test specimen for tensile, flexural and thermal tests.
3. Testing and analysing the 3D Printed structures for thermal and mechanical properties.
   - Thermal properties - thermal conductivity
   - Mechanical properties - tensile and flexural strengths.
4. Carrying out a computational analysis.
   - Heat transfer to compare the results which obtained from the experiments.
5. Proposing design recommendations
   - Optimizing the 3D printed polymer structures (FFF Method) for insulation applications.

1.3 Research questions

1. How do the thermal and mechanical properties vary with the different design configurations in 3D printed polymer honeycomb structures fabricated using Fused Fabricated?
2. What will be the relationship between structural design and fixing orientation to mechanical and thermal properties of the material?
3. What steps can be taken to optimize these properties for thermal insulation applications?

1.4 Limitations

In this research, fused filament fabrication method is used to fabricate insulation structures and mainly filaments are polymer materials. So, there is no comparison with other 3D printed technologies. Size of the structures is selected based on the parameters (especially dimensions) of testing equipment at the Arcada laboratory. Samples are made of PLA filaments only.

1.5 Theoretical framework

The research is based on different theoretical aspects, heat transfer concepts, thermal insulation principles, polymer materials, design of structures using SolidWorks software, testing of thermal and mechanical properties and insulation performance of 3D printed structures, additive manufacturing and Fused filament fabrication, sustainable.

1.6 Method

Method of this research lies several steps. Selection of process parameters, sample preparation (design of digital models and fabrication), experimental testing of thermal and mechanical properties, and data analysis are the main activities. A computational analysis helps to check the accuracy of the experimental method.

1.7 Compliance with the Degree Programme Theme

Material engineering, computer aided design, additive manufacturing, processing methods and optimisation, and sustainable design, heat transfer are the main areas of the degree programme, and this thesis aligns with these themes. Investigation of mechanical and thermal properties of 3D printed polymer structures using different parameters and materials is related with innovative material design and optimization. This research allows to get a deep understanding about advanced manufacturing techniques and to contribute valuable insights into creating more sustainable, application-specific materials. Thermal insulation applications are a complement 4 to the themes of energy efficiency and sustainability, which are becoming more crucial in modern engineering. The curriculum, academic objectives align with this research project, which is also strengthened my technical skills and supports the program's focus on creating sustainable solutions for particle engineering challenges.

Further, development of practical skills in additive manufacturing, experimental design and statical analysis, learning advanced AM techniques, design digital 3D structures with computer aided design and computer aided engineering software and improving the writing skills and present logically are other areas which can be improved via this thesis.

1.8 Disposition

To ensure the clarity and coherence of the thesis, content is represented in a logical flow, is known as the disposition which has been categorised mainly in seven chapters.

1. Background - This is described under several subheadings such as motivation for choice the topic, aim, objectives, questions, limitations, theory (brief description), method (brief description) and comply with the degree thesis.
2. Literature survey - A summary of the published works
3. Theoretical framework - All the relevant theories, testing and models are described under this chapter.
4. Methodology - This chapter describes the methods which are used to achieve the research objectives. A detail description about research design, materials, fabrication process, experimental setups, data analysis, sustainable approach and computational model.
5. Results and calculations- The data obtained from the experiments and simulations are presented under this chapter.
6. Discussion - This chapter is to summarize, critically examine and discuss the results.
7. Conclusion - summarize the key finding, understand the relationships with the objectives and suggest the area of future studies is included under this chapter

In addition to above chapter, title page, abstract, acknowledgements, table of contents, list of figures and tables and list of abbreviations are placed before the chapter 1 while, references and appendices are shown after the chapter 8.

2 Literature Review

The research was carried out to evaluate thermal and mechanical properties of different material and objects which were fabricated using different methods of additive manufacturing aiming different objectives. High thermal properties are very important in heat exchangers, heat dissipation, thermo-mechanical equipment etc. while low thermal material can be used for insulation purposes. The high strength and light weight structures are cost effective in the industries.

Several research projects were carried out to check weather how to increase the thermal properties of structures, which were fabricated using laser powder bed fusion method. AlSi10Mg lattice structures were tested to evaluate heat conduction properties and light weight criteria. In these studies, revealed that the thermal conductivity of the lattice structures can be increased by modification of the structure through heat treatments or increasing the minimum cross-section area along the main heat conduction direction [24, 25]. Kamata, M. et al [26] investigated to develop a thin flat loop heat pipe to heat dissipation under low temperatures in satellite with high effective thermal conductivity. The pipe was fabricated using metal additive manufacturing with Ti alloy. As per the findings, a 3 mm thick loop heat pipe showed a higher effective thermal conductivity of 6050-7730 W/ (m.K) and can be used for heat transferring in low temperature (from -45oC to 20oC). Orkhan Huseynov, Seymour Hasanov and Ismail Fidan [27] studied the influence of the matrix material on thermal properties of the short carbon fibre reinforced polymer composites (ABS, PETG, Nylon and PC/PBT with and without short carbon fibres). According to the results, it was revealed that the matrix material has high impact on the thermal conductivity and coefficient of thermal expansion, whereas the variation

of the glass transition temperature and specific heat capacity was not changed significantly compared to the neat polymer. The values of the experiments can be used as a database to predict thermal history. Panda, B. et al [28] investigated the effect of design parameters to the mechanical properties (yield strength and modulus) of 3D printed (FDM) honeycomb structures on experimental and numerical basis. ABS P400 material was used to fabricate samples with different wall thickness and cell sizes. By comparing the experimental and numerical (3 models) results, one numerical model was proposed as the best to perform 2D, 3D surface analysis. Yield strength (11.2 MPa) and elasticity modulus (0.311 MPa) which were obtained through uniaxial compression test were compared with the values which obtained from 3 models (genetic programming (GP), automated neural network search (ANS) and response surface regression (RSR)). ANS model, which was very close to original readings, can be recommended as the best model to analyse the mechanical properties. Another research project was done by Jiang, H. et al [29] to study infill strategies in honeycomb core and solid shell composite structures which were fabricated using FFF with carbon fibre reinforced Polyetheretherketone (CF-PEEK) and Hydroxyapatite reinforced Polyetheretherketone (HA-PEEK). Mechanical properties of the specimen were evaluated with the deposition paths which are very important in fabrication of bone for implant applications using additive manufacturing. This study proofed that the compression properties of the specimens were closely related to printing paths. When crossing the infill paths, it leads to create defects at the notches and reduce the strength of the specimen and non-crossing paths increase the strength of the specimen because lack of the defects.

Since, high thermal properties play an important role in heat management, several research projects were conducted based on 3D printed 3d structures with different materials to achieve high thermal properties. Alqahtani, S. et al [30] carried out research to study heat transfer mechanism in polymer lattice structures with air voids. The test specimens were fabricated using filament fabrication method with Nylon, PLA, ABS, PETG filaments in different shapes (triangular, diamond and hexagonal). Similar study was done by Alqahtani [31] but with six different lattice geometries to investigate the thermal and mechanical properties for energy saving applications in buildings. The both studies observed that the relative density of lattice structures and the sizes of a unit cell and the specimen affected significantly the U-value (thermal transmittance). The hydraulic diameter of the design of polymer-lattice structures should be less than 8mm only for a conductive mode of heat transfer. The effect of an AM process parameter (layer thickness and type of 3D printer) on the U-value of the polymer lattices was a mild effect. A scale to predict the U-value of polymer lattices based on effective thermal conductivity and the specimen's depth was proposed as per the results of the experiments. Taleb, O. et al [32] conducted a study on “Thermal conductivity of 3D-printed block-copolymer-inspired structures” related to heat dissipation. The impact of the geometries and volume fraction to thermal conductivity of structures (lamellar, gyroid, and cylindrical with different volume fractions) were examined. Outcomes were that thermal conductivity can be controlled by introducing air cavities and increasing geometrically complex of the designed blocks leads to enhance the thermal performance.

To cater the requirement of low thermal conductivity related to insulation purposes in building and other industries, research was carried out with the samples fabricated using

additive manufacturing, PLA material. De Rubeis, T. et al. Carried out 3 sets of research works with same set of samples (a multi-row structure, a square structure, a honeycomb structure) with 6 voids. The first study [33] was to compare the thermal performance, and the second study [34] was conducted by filling the air voids of the structures with polystyrene and wool. Comparison of results was done based on the readings of the test with empty block. In the third study [35], the air voids filled with wood sawdust, sheep's wool and hemp. Outcomes of three studies were quite similar; The shapes of the 3D-printed blocks reduced the flow of heat exchange and increasing the complexity could lead to the heat flow reduction. With the filling the voids, heat flow reduction was improved further by approximately 50%. Bahar, A. et al [36] studied about thermal and mechanical behaviour of PLA-wood composites to check the potential of using in building insulations. It was observed that printing process led to minor contraction of tensile strength and effect of printing temperature was negligible to the stiffness and engineering constant. Thermal properties significantly depended on infill rate. Further PLA-wood composite showed a positive trend in building insulation; Its performance was lesser than the glass wool by 38% to 57%. Pei, Y. et al [37] carried out research to analysis the thermal performance of vacuum insulation panels which can be used in building insulation. Testing was done with various vacuum levels. The outcome was the effective thermal conductivity of the VIPs, and the number of the interlayers was inversely proportional.

Anwajler, B. et al [38] researched on "The potential of 3D printing in thermal insulating composite materials" with the samples made of Thermoplastic polyester PET-G (polyethylene terephthalate-glycol) with different microstructure patterns. 3D model sample geometries were circular, square, triangular, hexagonal, Kelvin tetrahedron, gyroid, diamond and 2D Voronoi with different layers from 1 to 4. Selective laser sintering (SLS) and stereolithography (SLA) methods of 3D printing were used to fabricate composite samples. It was observed that the gyroid structure had the lowest thermal conductivity and it is like the thermal conductivity of mineral wool and polystyrene which are already used in the building industry. Increasing layer numbers of the panels significantly reduced the thermal conductivity. Li, S., Xin, J. and Chen, R. [39] studied on "Achieving high strength and low thermal conductivity: Additive manufacturing of mullite lightweight refractory" to check the thermal and mechanical properties of mullite lightweight refractory which was made of clay, alumina and fly ash. Through this study, it was observed that the compressive strength (4.3 MPa) could be improved while the thermal conductivity (0.58 W/m·K) could be decreased. Chung, S.-Y. et al [40] carried-out research to understand the effects of anisotropic voids on thermal properties of insulating media investigated using 3D printed (FFF) samples which cubed shape with different voids ratios, sizes and shapes. The result of the study said that anisotropic voids affected to reduce the thermal conductivity and can be used for insulation purposes. Forés-Garriga, A., Gómez-Gras, G. and Pérez, M.A [41] studied how infill density and geometry influence the mechanical and light weight of the structures. The elastic modulus and the maximum load decrease with the density of the pattern and mechanical properties relate to each sample's printing time. Based on the experimental data, validated numerical model was provided for predicting the compression stiffness of the different cell patterns with an average deviation below 5%.

A summarised details of theses under literature review are shown in table 1.

Table 1. Summary of theses under literature review

Ref.	Thesis	Aim	Printed method/ Material/Structure/ Variable
24	On the thermal conductivity of Alsi10mg and lattice structures made by laser powder bed fusion	Increase the thermal conductivity of AlSi10mg through heat treatment	- Laser Powder Bed Fusion - AlSi10mg - Gyroid matrix lattice - Volume fraction (0.2, 0.5)
25	Effective heat conduction evaluation of lattice structures from selective laser melting printing,	To evaluate the heat conduction performance of lattice structures used as lightweight materials in industries	- SLM - AlSi10mg - BCC, FCC and Octet-truss structures - Geometry with different struct radius and shapes, topology, porosity, specific surface area, cross-section area
26	Thermal performance of ammonia-based thin flat loop heat pipe fabricated by additive manufacturing	Development of a thin flat loop heat pipe (LHP) with high effective thermal conductivity	- Metal additive manufacturing - Ti alloy (Ti-6Al-4 V) - Thin pipe
27	'Influence of the matrix material on the thermal properties of the short carbon fibre reinforced polymer composites manufactured by material extrusion'	Present a detailed analysis of the matrix material effect on the thermal properties of the composites	-Fused filament fabrication -Short carbon fibre reinforced composites (ABS, PETG, Nylon and PC/PBT with and without short carbon fibres) - test specimen - different materials
28	'Experimental and numerical modelling of mechanical properties of 3D printed honeycomb structures	Study the effects of the design parameters on the mechanical properties (yield strength and modulus of elasticity)	-Fused deposition manufacturing -ABS P400 -Hexagonal honeycomb structures - different wall thickness and cell sizes.

29	Infill strategies for 3D-printed CF-peek/ha-peek honeycomb core-shell composite structures	The effect of deposition paths on the mechanical properties of the specimens were investigated	-Fused filament fabrication -CF-PEEK and HA-PEEK -Honeycomb core and solid shell - different disposition paths
30	Thermal performance of additively manufactured polymer lattices'	Study about the heat transfer mechanism in polymer-based lattice structures with enclosed air cavities and propose a scaling law to predict U-value of lattice structures.	-Fused deposition manufacturing -Nylon, PLA, ABS, PETG -Triangle, diamond and hexagonal lattice structures -Material, geometry
31	The effect of lattice topology on the thermal and mechanical performance of additively manufactured polymer lattices	To access the impact of lattice topology and variation in the number of unit cells on the K-value, U-value and compression strength of additively manufactured (AM) polymer lattice.	-Fused deposition manufacturing -PLA -Triangle, diamond, honeycomb, star, cubic, and gyroid -Geometry, volume percentage
32	Thermal conductivity of 3D-printed block-copolymer-inspired structures	Examining the impact that geometric structure, volume percentage and material combination has on thermal conductivity	-Fused filament fabrication -PLA -Lamellar, gyroid, cylindrical -Geometry, volume percentage
33	The 3D printing Potential for heat flow optimization: Influence of block geometries on heat transfer processes	To compare the thermal performance of three 3D-printed PLA blocks, characterized by different internal geometries and air cavities	-Fused deposition manufacturing -PLA -Multi-row structure, square structure, honeycomb structure -Geometry
34	3D-Printed Blocks: thermal performance analysis and	-To propose a new 3D-printed block to be used as thermal insulation of building walls, also considering	-Fused deposition manufacturing -PLA -Blocks with cavities

	opportunities for insulating materials	criticalities and potentials related to its realization -To analyse the thermal performance of the prototype 3D-printed block via theoretical and experimental approaches (by means of InfraRed Thermography (IRT) technique and Heat Flow Meter (HFM) method in Hot Box apparatus) -To evaluate the thermal performance of the 3D-printed block by filling its air cavities with waste materials, thus implementing the concept of circular economy.	-Different cavity filling materials (polystyrene, wool)
35	On the Use of Waste Materials for Thermal Improvement of 3D-Printed Block—An Experimental Comparison	To compare the thermal performance of a PLA 3D printed block with an internal honeycomb structure whose air cavities are filled with natural and recyclable waste-insulating materials	-Fused deposition manufacturing -PLA - Blocks with cavities -Different cavity filling materials (Wood sawdust, sheep's wool, hemp)
36	The thermal and mechanical behaviour of Wood-PLA composites processed by additive manufacturing for building insulation	To reveal the potential of using wood-PLA as a rigid insulator in the building sector for which the local control of the thermal properties is ensured by AM.	-Fused filament fabrication -PLA- wood composites - Crossed shape structure - Infill percentage (from 10% to 40%)
37	Experimental and theoretical thermal performance analysis of	Feasibility analysis of additive manufacturing technique to	- Fused filament fabrication - Black PLA - Vacuum panels -Vacuum pressure

	additively manufactured polymer vacuum insulation panels'	manufacture polymer VIPs.	
38	The potential of 3D printing in thermal insulating composite materials- experimental determination of the impact of the geometry on thermal resistance	-To analyse printed samples of prototype thermal insulation composite structures -To evaluate the thermal and mechanical properties	- SLS, SLA - Thermoplastic powder, resin - Circular, square, triangular, hexagonal, Kelvin tetrahedron, gyroid, diamond, 2D Voronoi \ -Geometry
39	Achieving high strength and low thermal conductivity: Additive manufacturing of mullite lightweight refractory	Study of thermal and mechanical properties of mullite lightweight insulation refractory	-Direct ink writing (DIW) -Clay, alumina, fly-ash -Specimen bar -
40	'Effects of anisotropic voids on thermal properties of insulating media investigated using 3D printed samples	To examine the effect of anisotropic voids on the thermal conductivity and direction modulus of an insulating medium	- Fused filament fabrication -ABS -Cubes with anisotropic voids - different void ratios, sizes, shapes
41	Mechanical performance of additively manufactured lightweight cellular solids: Influence of cell pattern and relative density on the printing time and compression behaviour	To investigate the role of the infill density together with the pattern geometry on the mechanical performance and weight reduction of cellular solids manufactured by FFF	- Fused filament fabrication -PEI U1tem 9085 - 2D cell shapes- Antitetrachiral, Circular, Hexachiral, Hexagon, Re-Entrant Hexagon type I and II, Lozenge Grids, Rotachiral, Sinusoidal Ligaments, Square Grids, SrCuBO, and Tetrachiral -Infill density, geometry

Based on the reviewed literature, the Fused Filament Fabrication (FFF) method and PLA material have been the most frequently studied. Common research themes include the effects of geometry, void areas, and infill percentages. However, the influence of void orientation within PLA blocks produced by the FFF method has received limited attention. To address this gap, the present study investigates the impact of different

geometries and void orientations—specifically in horizontal and vertical directions—on blocks fabricated using Hyper PLA filament through the FFF process to mechanical and thermal properties.

3 Theory

There are several theories behind this thesis such as Computer aided design, Computer aided Engineering, 3D printing, Heat transfer of materials and Mechanical behaviours of materials.

3.1 Computer aided design

Computer aided design (CAD) means that software which is used to create a digital 2D drawings or 3D models and technical illustrations of a product or a structure. First it was invented by Dr. Samuel Geisberg in 1985 which is known as Creo today, and onward many types of software are available such as AutoCAD, SolidWorks, CATIA, Fusion 360 and Rhino etc. Advantages of using CAD software are saving time, increase productivity, accurate designing and simplifying communication with clients or people who work with and integrating with computer aided manufacturing and computer aided engineering packages etc. [42,43,44,45].

Here SolidWorks, was discussed deeply because, it has been used to design digital samples.

SolidWorks

Basically, SolidWorks has been built for 3D designing widely used in the mechanical engineering purposes. 2D modelling also can be done with this software. SolidWorks software is used by professionals, manufacturers, students around the world for research, innovative design, speed, efficiency and accurate manufacturing, learning and teaching aspects. It is powerful, user-friendly and easy to learn. Models can be created as parts or assemble. A large or complicate object can be created assembling parts. Detailed drawings of the parts or assemblies can be prepared with SolidWorks with 2D or 3D views [46, 47].

3.2 Compute Aided Engineering

Computer Aided Engineering (CAE) software is used to support engineering tasks such as simulation, analysis, design validation and optimization etc. Different type of analysing tools such as finite element analysis (FEA), computational fluid dynamics (CFD), and multi-disciplinary design optimization (MDO) which assist to create prototypes and analyse designs. The design created by CAD can be uploaded into CAE software or can be created objects by itself for analysing. Advantages of CAÈ are product development with identification of potential issues can be done through digital prototyping and it leads to save time and money, analysis and optimization help to improve the quality and

accuracy of the products etc. Finite element method (FEM) has been practically applied in FEA tool to modelling and simulation of structural, acoustic, electromagnet or thermal performance of products. Common CAE software tools are ANSYS, Abaqus, SolidWorks simulation, COMSOL Multiphysics, Altair HyperWorks, Siemens NX etc. [48, 49, 50]. COMSOL Multiphysics is only discussed here because it was used for simulation the heat transfer phenomenon. Simulation step in CAD is shown in figure 3.

COMSOL Multiphysics simulation software

COMSOL is a developed mathematical modelling software with an ability to single or couple multiple physics phenomena in one simulation environment. COMSOL is used by engineers, researchers, scientists, manufacturers, teachers and learners to model and solve complex problems in different fields such structural mechanics, electrical (AC/DC), radio frequency, fluid, chemical, and thermal systems. User can apply the requirements such as defined geometries, physics, materials, and meshes, through model builder. After compute the model, results can be obtained [51, 52, 53].

COMSOL Multiphysics employs the energy conservation theory (first law of thermodynamics) to model the heat transfer in solids.

The governing equation for heat transfer in solid is,

$$\rho C_p \partial T/\partial t = \Delta(k.\Delta t) + Q$$

Where:

$\rho = density\ of\ material\ in\ \frac{kg}{m^3}$

$C_p = specipic\ heat\ at\ constant\ pressure\ inc\ \frac{J}{kg.K}$

$T = Temperature\ in\ K$

$k = Thermal\ Conductivity\ in\ \frac{W}{m.K}$

$Q = heat\ source\ in\ \frac{W}{m^3}$

$\Delta(k.\Delta t) = dheat\ conduction\ term(Fourier's law)$

This is a time dependent equation and for steady state condition, $\frac{\partial T}{\partial t} = 0$

Hence, $\Delta(k.\Delta t) + Q = 0$

3.3 3D printing

3D printing is known as additive manufacturing that builds parts layer by layer, eliminating the need for moulds. With 3D printing, it is easy to create complex geometries that are often difficult or impossible to do with traditional methods. This process offers

several benefits such as low start-up costs, very low start-up costs, very quick turnaround, large range of available materials, design freedom at no extra cost, each part can easily be customized, less wastage etc. 3D printing is best for low volumes, complex designs and rapid design. History of 3D printing goes to 1980s. The patent for 3D printing was obtained by Chuck Hull in 1984 [54]

There are different types of process according to the different type of materials such as Vat Polymerization (for liquid photopolymer), Material extrusion (for thermoplastic), Powder bed fusion (for powder particles), Material Jetting (droplets of liquid), Binder Jetting (droplets of liquid), Direct Energy Deposition (for molten metal), Sheet Lamination (individual sheets) [55, 56]. These methods are categorized in figure 1.

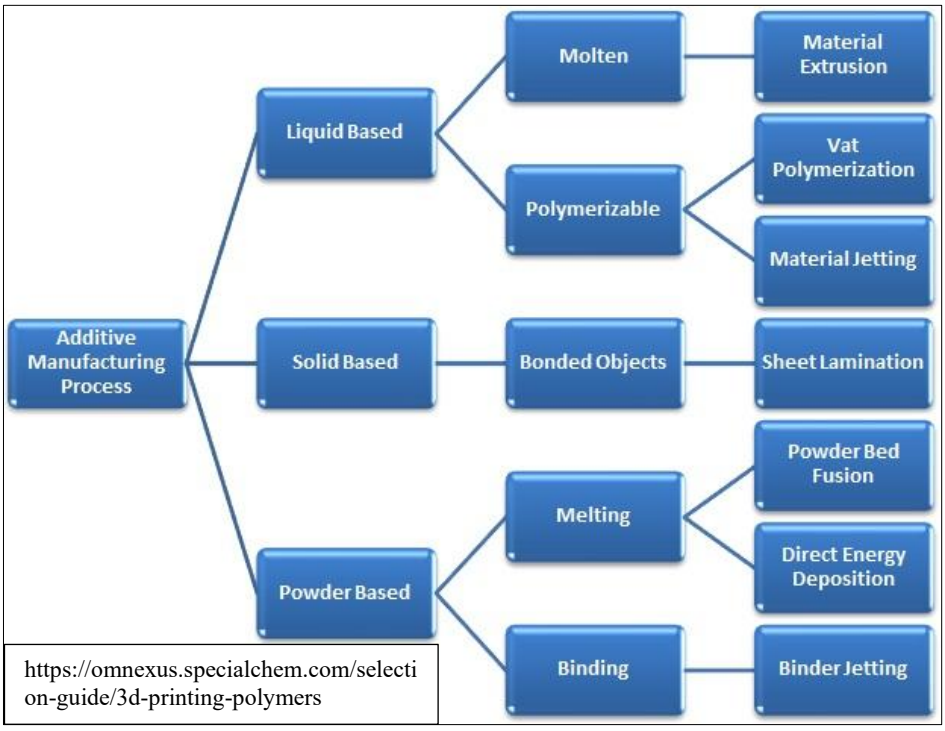

Figure 1. 3D printing methods

Material Extrusion is a broad category of 3D printing such as fused filament fabrication (thermoplastic filaments), direct ink writing (viscous pastes, gels or inks), pellet extrusion. Fused Filament fabrication is only discussed here because it will be used for sample fabrication [57].

Fused Filament Fabrications

Fused filament fabrication (FFF) is a widely used method for printing with thermoplastic filaments; a melted filament material is extruded through a heated nozzle to create an object layer by layer. The process of FFF (figure 5) and printing of an object with extrusion method (figure 2) are shown below.

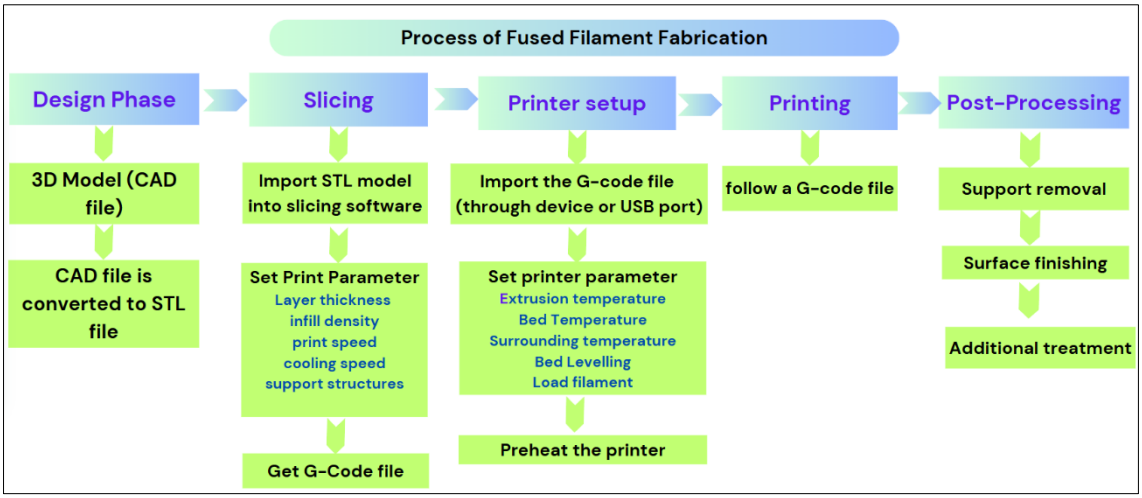

Figure 2. Process of Fused Filament Fabrication

3.4 Thermal Conductivity

Thermal conductivity helps to identify the thermal behaviour of materials. The materials which have higher thermal conductivity, have great ability to transmit heat. Hence, thermal conductivity plays a vital role in design and the selection of materials. For instance, low thermal conductivity materials such as foam are normally used in thermal insulation purposes. Heat transfer occurs in three ways, conduction through solids, convection through air or liquid and radiation (without media). It is considered that convection is not happening, and the radiation is neglected when finding the thermal conductivity [58,]

Thermal conductivity describes that the ability of a material to transfer or conduct heat through itself. Mathematically, it can be defined as the rate of heat energy transmitted through a unit area of material due to a heat gradient (unit) is quantified by thermal conductivity, which is a fundamental material property [59,60].

It is expressed by an equation known as Fourier's Law of Heat Conduction. The minus (-) sign shows the direction of flow. Figure 3 illustrates the heat transferring phenomenon through an object.

$$q'' = -k * \frac{dT}{dx}$$

Where:

$$\frac{dT}{dx} = Temperature\ gradient\ in\ \frac{K}{m}$$

$$k = Thermal\ Conductivity\ in\ \frac{W}{m.K}$$

$$q'' = heat\ flux\ in\ \frac{W}{m^2} = \frac{Q}{A}$$

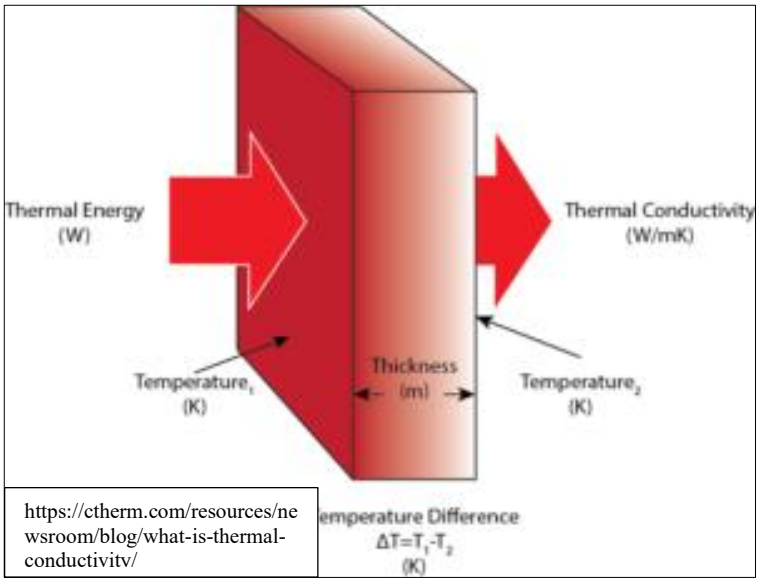

Figure 3. heat transferring phenomenon through an object

In initial stage, temperature increases with the time and after a considerable time period, the temperature reaches a fixed value. It means the temperature gradient is zero and the steady state is achieved. The figure 4 shows the temperature changing in steady state.

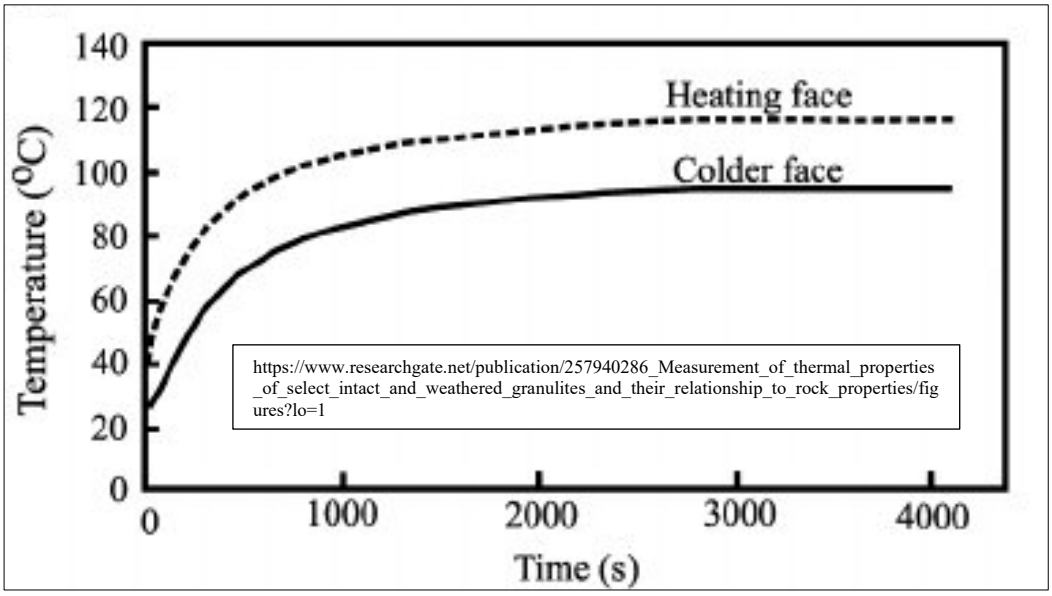

Figure 4. Temperature changing in steady state

The equation derived for thermal conductivity for steady state

$$k = \frac{q'' * L}{T_1 - T_2} = \frac{Q * L}{A(T1 - T2)}$$

Where:

$Q = Heat\ source\ in\ \frac{W}{m^3}$

$L = Thickness\ in\ m$

$T1\ \&\ T2 = Temperatures\ at\ heated\ surface\ \ and\ cold\ surface\ in\ K$

$A = Area\ in\ m^2$

When the heat source is supplied by an electric power source, q'' can be found by the relationship between **Voltage (V)**, and **Current (I)** with the known heat source which is used in the experiment. Voltage, Current and temperature difference can be taken from the experiment for each block.

$$q'' = \frac{V * I}{A}$$

$$k = \frac{V * I * L}{A(T_1 - T_2)}$$

Thermal conductivity can be obtained experimentally by the steady state heat conduction test.

3.5 Tensile strength

Tensile strength is one of the key mechanical properties which is used to evaluate the performance of a substance in applications such as structural elements, etc. Tensile strength of material describes that how much force the material can take across its area before it gets permanently stretched or broke. Another way, the maximum tensile stress can be borne by a material before its failure [61].

It is expressed as

$$\sigma_t = \frac{F_{max}}{A_0}$$

Where:

$\sigma_t =$ Tensile stress in MPa

$F =$ maximum force applied before breaking in N

$A_0 =$ ínitial cross section in mm^2

The tensile strength equals to the stress at the failure point of the material.

Tensile strength can be tested by tensile test with the universal tensile testing machine for any material with standard test specimens. A typical stress vs. strain curve is shown in figure 5. There are two types of deformations: plastic and elastic. The region before the yield point is known as elastic region. The yield strength (A), Ultimate strength (B) and breaking strength (C) can be obtained from the graph directly. The young modulus can be calculated by the linear part of the graph, the slope of the line in elastic region [62, 63].

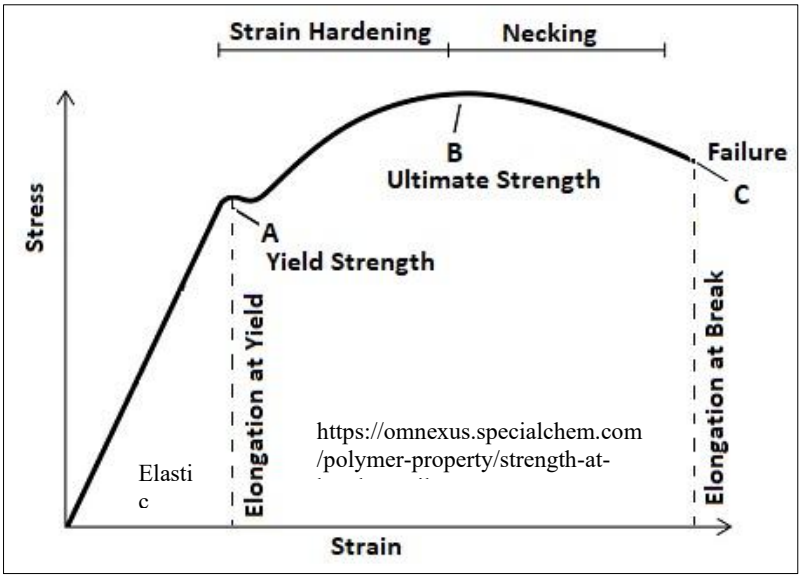

Figure 5. A typical stress vs strain curve

Shape of the stress vs. strain curve is changed from material to material. For some materials, it is not easy to recognize the changing from elastic to plastic. In such cases, 0.2% offset yield strength method is used [64].

0.2% offset yield strength method

First, the stress strain curve is graphed with excel sheet. Then young modulus (E) can be got according to the linear part of the path. Then 0.2% of the strain is added to original strain, and after that 0.2% offset stress is calculated by multiplying original strain values and calculated young modulus.

$$0.2\%\ offset\ strain = Original\ strain + 0.2\%\ Original\ strain$$

$$0.2\%\ offset\ yield\ stress = Original\ strain * Young\ modulus$$

Then plot the 0.2 % offset stress strain graph. The meeting point of original curve and offset line gives yield strength. It is graphically represented in figure 6.

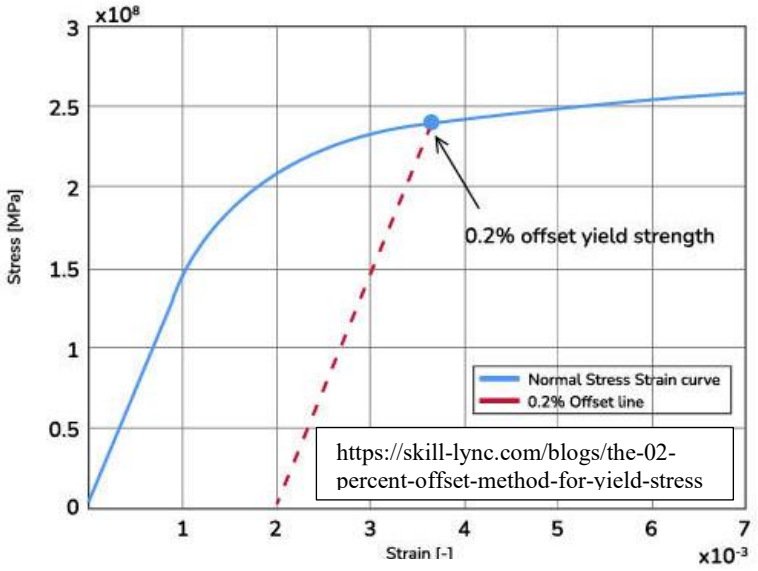

Figure 6. 0,2% off-set line

3.6 Flexural strength

Flexural strength describes the behaviour of a material under stress before it bent or broke. It helps to understand about the durability and resistance of material which are essential for product design and structural engineering. It is Flexural stress before it bent or broke equals to flexural strength [65, 66].

The flexural strength can be evaluated by flexural test with the universal flexural test machine with 3 bending tests. Flexural test specimen was tested with 3 point bending test for this study and the theory behind that test is as follows [67]. The loading arrangement is shown in figure 7.

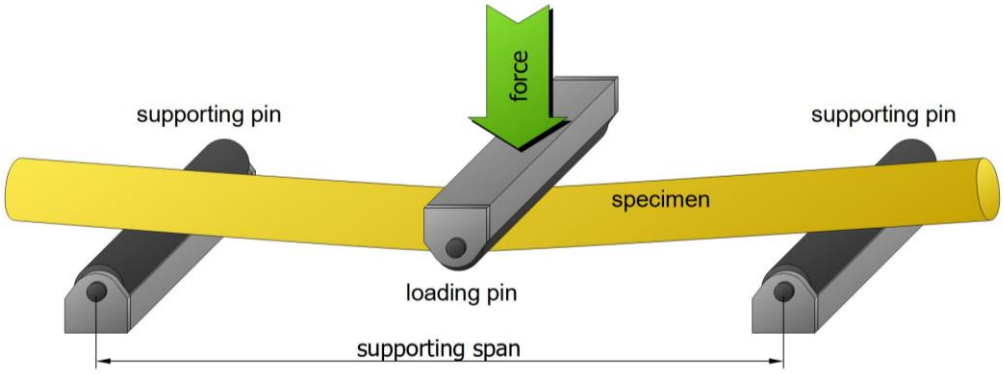

https://www.tec-science.com/material-science/material-testing/bending-flexural-test/

Figure 7. Three (3) points flexural test arrangement

Flexural stress

Flexural stress (or bending stress) is the ability of a material to resist deformation under flexural load. It is expressed as

$$\sigma_f = \frac{3FL}{2bh^2}$$

Where:

$\sigma_f = flexural\ stress\ (MPa\ or\ N/mm2)$

$F = maximum\ force\ applied\ before\ breaking\ in\ N$
$L = supporting\ length\ in\ mm$
$b = width\ of\ the\ specimen\ in\ mm$
$h = thickness\ of\ the\ specimen\ in\ mm$

Flexural strain

Flexural strain is the amount of deformation of a material occurs under bending before it yields. It is expressed by

$$\varepsilon_f = \frac{6sh}{L^2}$$

Where:

$\varepsilon_f =$ flexural $strain$
$s = deflection\ of\ the\ specimen\ in$ mm
$L = supporting\ length\ in\ mm$
$h = thickness\ of\ the\ specimen\ in\ mm$

Flexural modulus

Flexural modulus is the stiffness of the material when it is bent. It is expressed by

$$E_f = \frac{\sigma_{f2} - \sigma_{f1}}{\varepsilon_{f2} - \varepsilon_{f1}}$$

$$s_i = \frac{\varepsilon_{fi} L^2}{6h}$$

$$\varepsilon_{fi} = 1\ or\ 2\ and\ \ then\ \varepsilon_{f1} = 0.005\ and\ \varepsilon_{f2} = 0.0025$$

Where:

$s_i = deflection\ in\ mm\ for$ 1 & 2
$\varepsilon_{fi} = flexural\ strain\ for$ 1 & 2
$L = supporting\ length\ in\ mm$
$h = thickness\ of\ the\ specimen\ in\ mm$
$E_f = flexural\ modulus\ in\ MPa$
$\sigma_{fi} = flexural\ stress\ in\ \ MPa\ for$ 1 & 2

4 Methodology

This is an experimental based study for evaluation of thermal and mechanical properties of four samples. Main steps are creating digital models and test specimens with SolidWorks, then fabrication of them through fused filament fabrication method. Then steady-state heat conduction test, tensile test and flexural test were carried out. Based on the experimental data, calculation was carried out to obtain the values for thermal conductivity, young modulus, yield strength, tensile strength, flexural modulus and flexural strength.

4.1 Sample Design

Different designs have been used in previous thesis [68, 69] for Honeycomb structures with various shapes such as triangle, square, hexagonal, etc. To deviate from the previously used designed, own patterns were created with triangle (design 1) and circles

(design 2). Dimensions of the longest element of the design are less than 5,5 mm. The design 1 has an evenly spread design over the area, but design 2 is not evenly distributed. The two patterns are shown in figure 8.

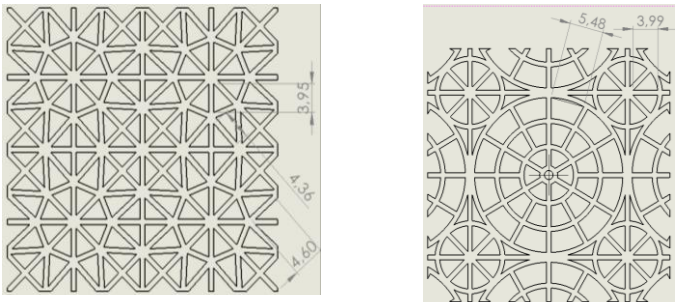

Design 1 *Design 2*

Figure 8. Patterns for honeycomb

Each design has two configurations, which is called as horizontal and vertical. The direction which is perpendicular to the design is called as horizontal while align to the design is called as vertical as shown in the figure 12. Due to these different orientations and patterns give the different inner geometries to the structures.

The four models were named as Design 1 horizontal, Design 1 vertical, Design 2 horizontal and Design 2 vertical. The horizontal and vertical directions are clearly shown in figure 9.

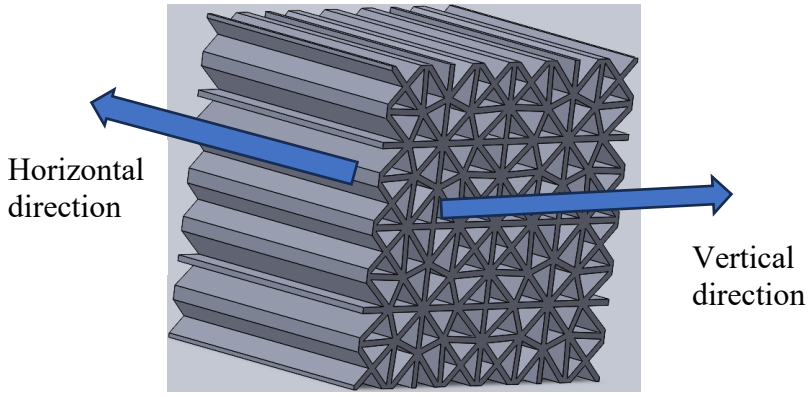

Figure 9. Horizontal and vertical directions of samples

Design of test specimen

For testing of thermal conductivity blocks in dimension 39.25 mm x 39.25mm x 32 mm were designed for each design and direction. The designed specimens were shown in the figure 10.

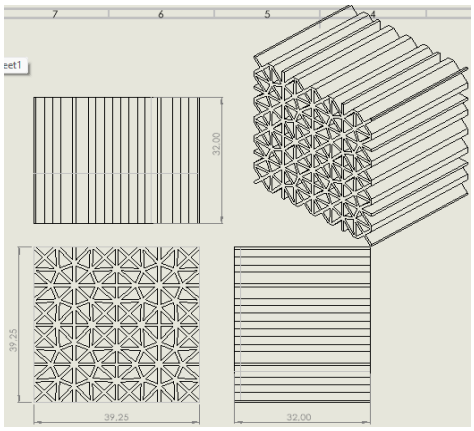

Design 1

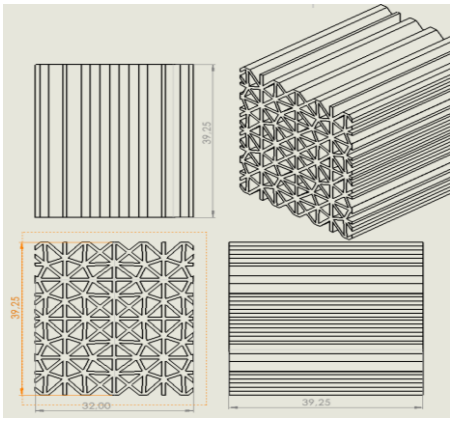

Design 1 Vertical

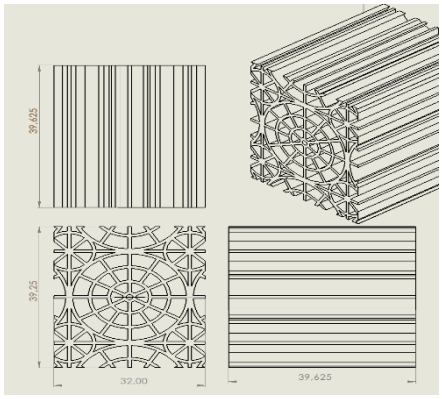

Design 2

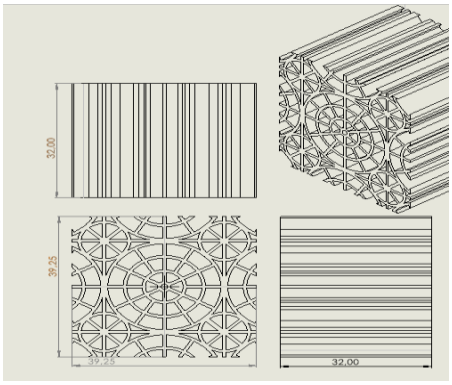

Design 2 Vertical

Figure 10 Horizontal and vertical directions of samples

Test specimens have been created from above design structures for tensile testing. The size and shape of the structures are according to the code ISO 527. The dimension of the samples is 170mm x 20mm x 4mm, but the actual specimen sizes are deviated by these dimensions because a 0.8mm thick outer skin layer is proposed to cover the samples to get a smooth finish. So, the thickness is increased by 0.8 mm overall of the specimen in all directions than the ISO 527 In figure 11 shows the specimen sizes with the outer skin.

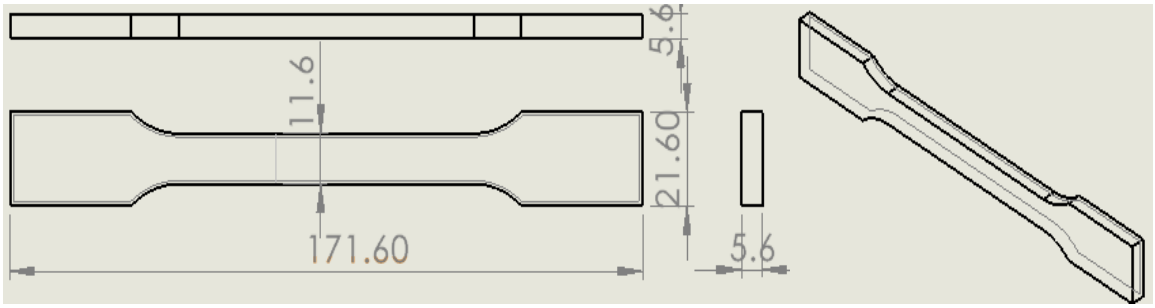

Figure 11. Specimen for testing tensile strength

Test specimens for flexural testing were designs according to the code ISO 178. The dimension of the samples 80mm x 10mm x 4mm for flexural strength. Similarly to the tensile specimens, an outer skin was introduced, and the final specimen size was 81.6 mm x 11.6 mm x 5.6 mm. The specimen is shown in figure 12.

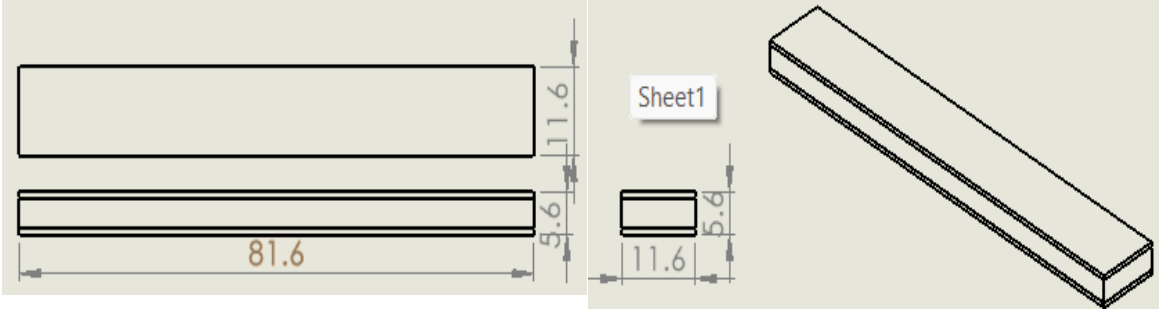

Figure 12. Specimen for testing flexural strength

When creating the specimens, always it was considered the same area of the pattern to maintain a unique pattern. The considered areas are highlighted in figure 13.

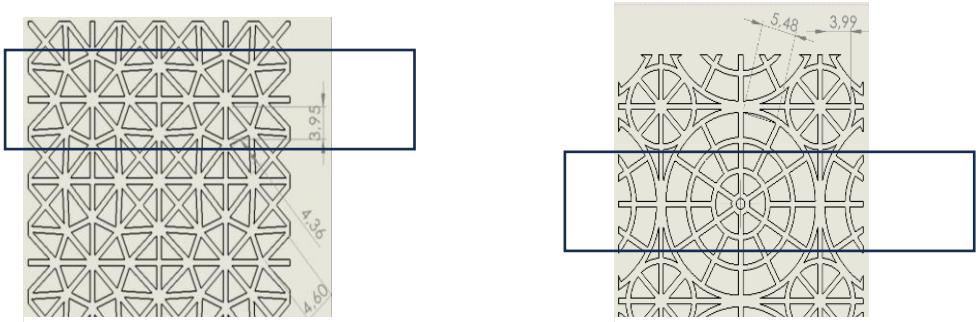

Design 1 *Design 2*

Figure 13. Areas for creating specimens

4.2 Sample Fabrication

The samples were printed by Fused Filament fabrication of 3D printing technology with Hyper PLA filaments with the slicing software - Creality Print 6, and the printer - Creality K2 plus. The SolidWorks files were converted STL files and then the STL files were opened through slicing software with 100% infill density, 200 mm/s speed and 0.2 mm layer thickness.

After that, the slicing, files were saved as g-code files. These g-code files were opened in Creality K2 plus printer with the preheated parameters of 220 °C extrusion temperature, 53 °C bed temperature and 34 °C surrounding temperature and started to print. The fan speed for first 1-3 layers was 0-30%, and after that it was 100%. To ensure the better bond between bed and the object cooling speed was in low value in the beginning. Figure 14 shows the arrangement of slicing and printing processes.

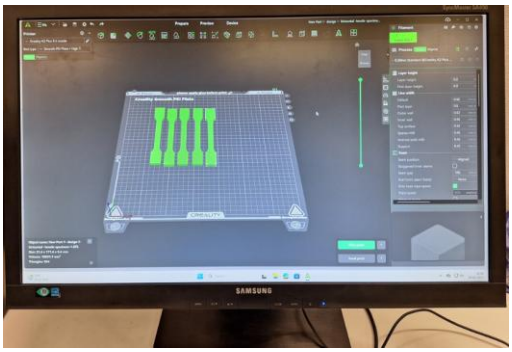

Slicing

Printing

Figure 14. Slicing and printing processes

l totally 40 numbers for tensile and flexural testing. Four numbers of honeycomb structures (1 for each) for thermal conductivity test were printed.

4.3 Thermal and Mechanical testing

Testing was carried out for finding thermal conductivity, tensile strength and flexural strength, modulus etc.

4.3.1 Thermal conductivity

Steady-state heat conduction tests were used for testing. First the apparatus, heat source, voltmeter, ammeter, connection cables, Amprobe T-56 device, T-56 software installed computer, sample, two thermocouples, heat plate, air control chamber etc. was arranged to measure the temperature of top surface and bottom surface of the sample as shown in figure 15 (a-d).

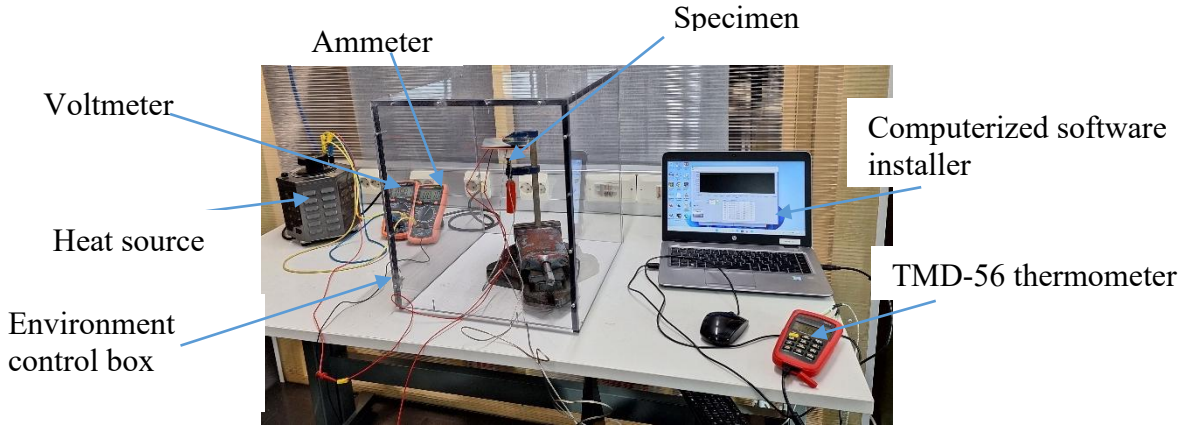

a) Arrangement of Test apparatus

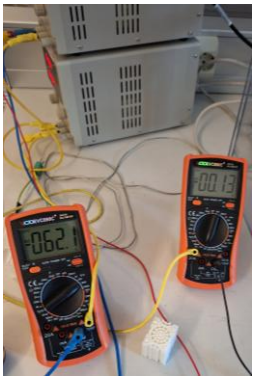
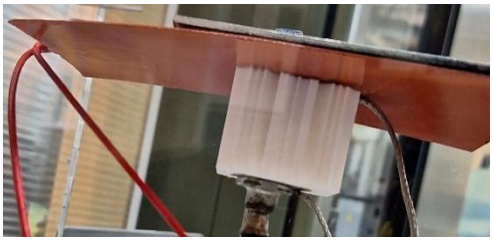


b) Heat source, voltmeter and ammeter

c) Sample fixing

d) Thermometer and software

Figure 15. Arrangement of Test apparatus for thermal conductivity test

The voltmeter and ammeter were connected to the heat source, and then heat source and ammeter related to the heat plate through connection cables (figure 7 b). Top side of the sample was connected to the heat plate to receive the heat to the sample (figure 7 c), and both top and bottom sides related to the TMD-56 device which related to the computer. The sample area was covered by a chamber to maintain a constant environment to prevent convection.

The heat source was switched on and readings of the voltmeter (62.1 V) and ammeter (0.13 A) were recorded. The software was used to monitor the temperature at heat surface (T1) and temperature at cold surface (T2) and visualize the data through graphs. The test continued until reaching the steady state condition. Finally, the recorded temperatures were exported as an Excel file. The procedure was repeated for four samples.

4.3.2 Tensile strength

Testometric X350-20 machine used for testing. It is a universal testing machine with WinTest Analysis EC software package which is allowed to carry out full PC control and create and store test data [70]. The procedure was followed as per the code ISO 527.

First installed the grips for tensile testing and then set the parameters such as maximum load, starting position, and return position after finishing the testing, speed (10 mm/min), data acquisition etc. The specimens were clamped into the grips and started the test. The PC which is installed the software continuously recorded the force, elongation and time and showed them as a graph. The result is recorded as a CSV file and PDF formats. The test was repeated for four samples by testing 5 specimens per each. Fixing arrangement of the tensile test is shown in figure 16. The procedure was followed as per the code ISO 527.

Figure 16. Fixing arrangement of tensile test

4.3.3 Flexural strength

The Universal testing machine with two lower and one upper supports. Similarly to the tensile test, after setting the parameters, sample was fixed horizontally over the lower 2 supports and started the test. While test was conducted, force, deflection and time could be monitored through the monitor. Finally, the results for all specimens were taken as CSV and PDF formats. Fixing arrangement of the flexural test is shown in figure 17. The procedure was followed as per the code ISO 179.

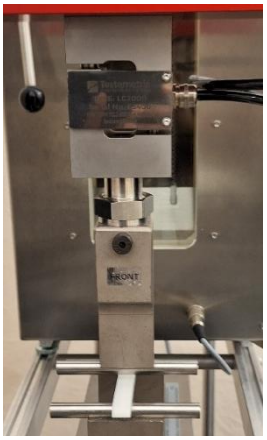

Figure 17. Fixing arrangement of flexural test

5 Results and calculations

5.1 Thermal conductivity and diffusivity

Test data recorded for about four hours for one test, but here recoded data is displayed for first 15
s for illustration in table 2. Test data of the temperature at heated surface (T1) and temperature at cold surface (T2) with respect to time was tabulated in table 2.

Table 2. Results from thermal conductivity tests

Time	D1 H	D2H	D1V	D2V	D1H	D2H	D1V	D2V
(s)	T1 (deg C)				T2 (deg C)			
1	23,6	24,5	33,1	24,4	21	23,4	21,8	22,6
2	23,6	24,5	33,1	24,4	21	23,4	21,8	22,6
3	23,7	24,6	33,1	24,4	21	23,4	21,8	22,6
4	23,7	24,7	33,2	24,6	21	23,4	21,8	22,6
5	23,7	24,7	33,2	24,6	21	23,4	21,8	22,6
6	23,7	24,8	33,3	24,6	21	23,4	21,8	22,6
7	23,9	24,8	33,3	24,6	21	23,4	21,8	22,6
8	23,9	24,9	33,3	24,7	21	23,4	21,8	22,6
9	23,9	24,9	33,4	24,8	21	23,4	21,8	22,6
10	23,9	25	33,4	24,8	21	23,4	21,8	22,6
11	24	25	33,4	24,8	21	23,4	21,8	22,6
12	24,1	25	33,4	24,9	21	23,4	21,8	22,6
13	24,1	25,1	33,4	24,9	21	23,4	21,8	22,6
14	24,2	25,1	33,5	25	21	23,4	21,8	22,6
15	24,2	25,2	33,6	25	21	23,4	21,8	22,6

The graphs, the temperature at heated surface (T1) vs. time and temperature at cold surface (T2) vs time were presented in figure 10 for all cases in figure 18.

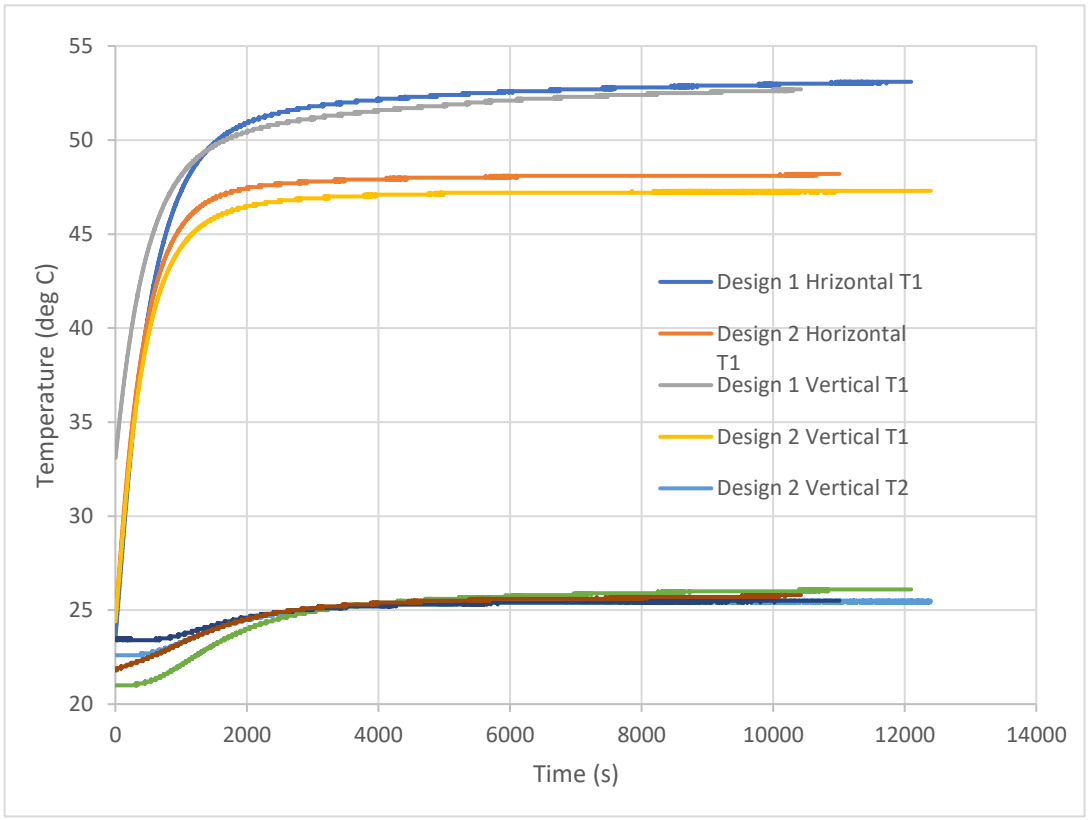

Figure 18. Graph for T1 and T2 vs Time for all cases

To more clearly visualize the temperature differences, individual graphs are shown in figure 19 a, 19 b, 19 c and 19 d.

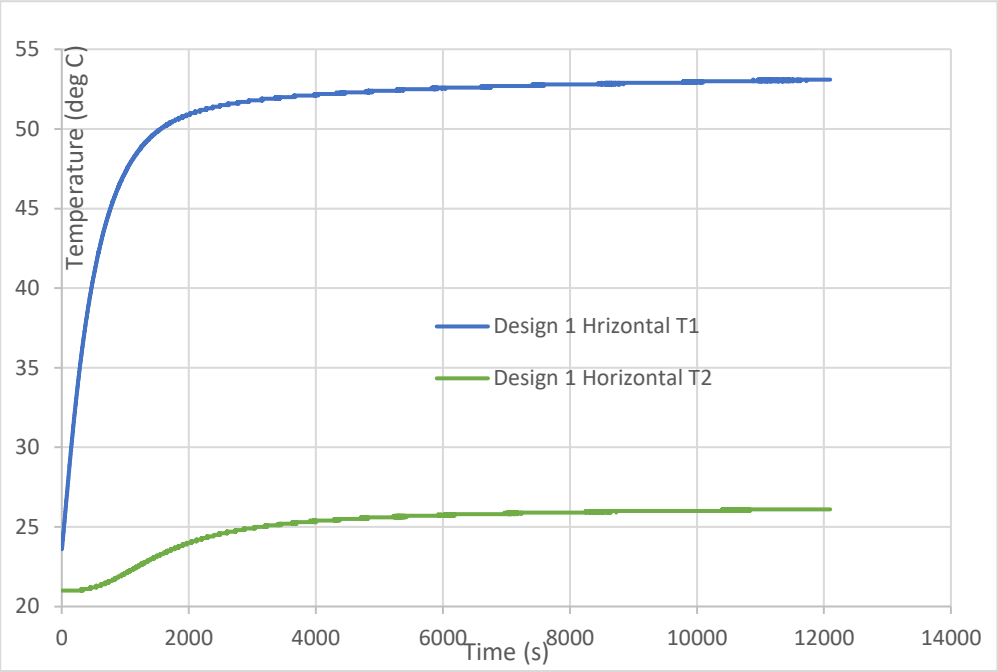

Figure 19 a. Graph for T1 and T2 vs Time for D1H

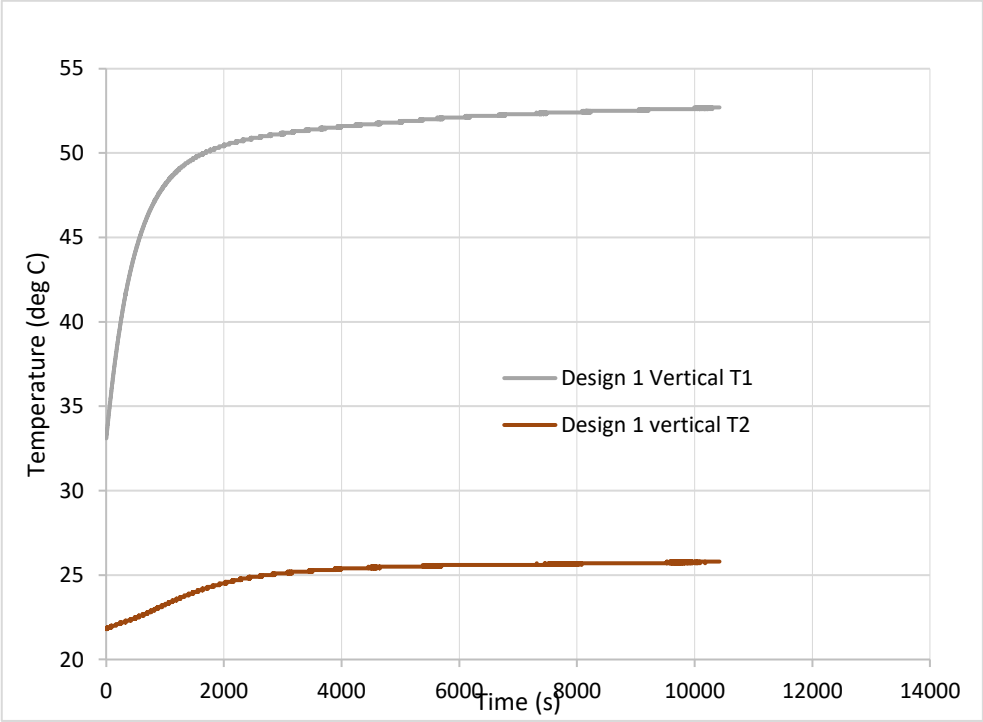

Figure 19 b. Graph for T1and T2 vs Time for D1V.

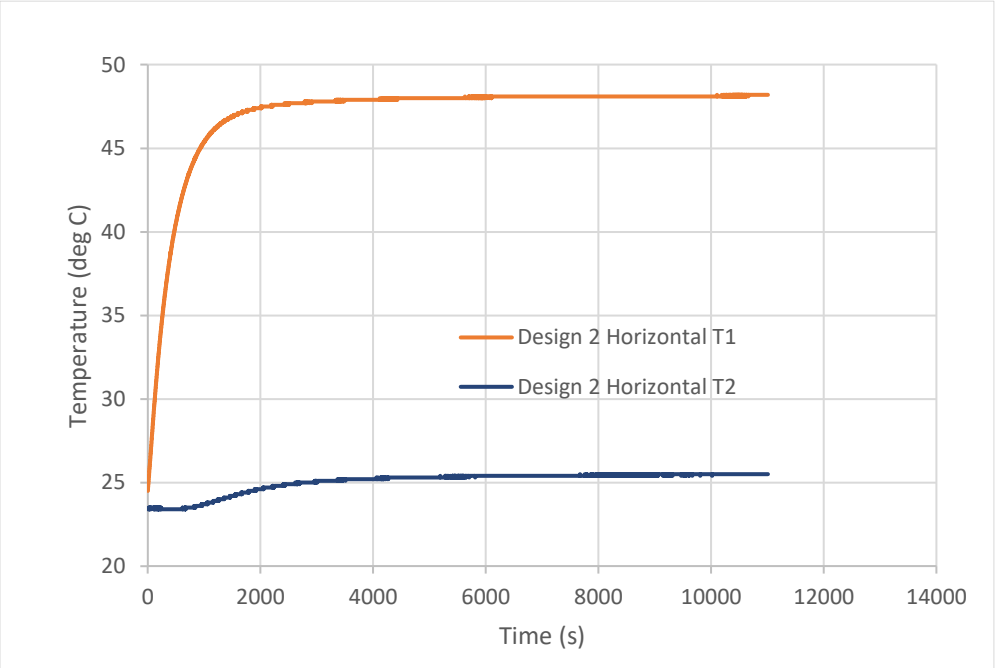

Figure 19 c. Graph for T1and T2 vs Time for D2H.

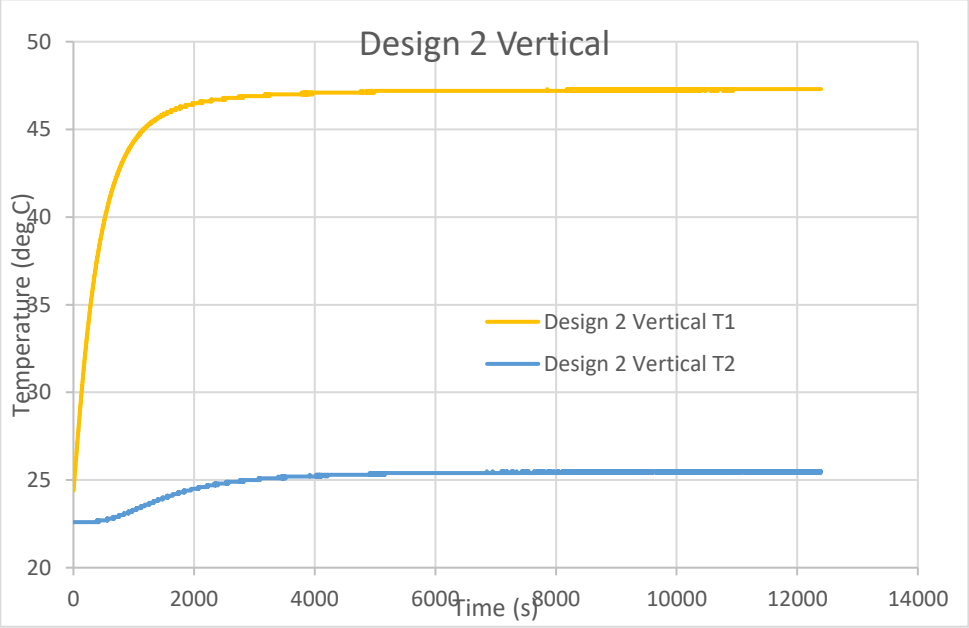

Figure 19 d. Graph for T1and T2 vs Time for D2V.

Considering the steady state condition, thermal conductivity was calculated using the equation mentioned in chapter 3.3.1.

Temperatures at steady state for all samples and test parameters are in the table 3.

Table 3. Calculation of Thermal Conductivity

Voltage (V)	=	62,1	V	Thermal conductivity $k = \frac{V * I * L}{A(T_1 - T_2)}$
Current (I)	=	0,13	A	
Area (A)	=	1540,56	mm^2	
Thickness (L)	=	32	mm	

Sample	T1 °C	T2 °C	Thermal Conductivity (k) (W/K.m)
Design 1 Horizontal	53,1	26,1	6,211
Design 1 Vertical	52,7	25,8	6,234
Design 2 Horizontal	48,2	25,5	7,387
Design 2 Vertical	47,3	25,4	7,657

5.2 Tensile strength

All the tested data were obtained as pdf files and as CSV files separately for each test. The CSV files used for calculations which were done using excel spreadsheets, because it was very easy to draw graphs. The yield point of the curves could not be recognized at once; therefore 0,002 offset method was used. The original graph and the 0,002 offset line were drawn in same graph, and the intersection point of the two paths was taken as the yield point. Considering the linear part of the curve, gradient of the elastic region was calculated, and it was taken as young modulus which was used to calculate 0.002 stress value. The value of the maximum original stress was taken as ultimate tensile strength.

The calculation of original stress and strain is illustrated in table 4.

Table 4. Calculations of strain and stress using data in CSV file (Design 1 – horizontal tensile specimen 1)

Calculation of stress and strain				
Area		a =	64,96	mm^2
Initial length		Lo =	115	mm
strain = elongation /initial length stress = force/area				
From the CSV file			Calculations	
Force (N)	Elongation(mm)	time (s)	Strain	Stress
17,9	0	0,02092	0	0,275554
17,9	0,000679	0,040989	5,90E-06	0,275554
18	0,00206	0,060977	1,79E-05	0,277094
18,5	0,004164	0,080969	3,62E-05	0,284791
19,7	0,007045	0,100946	6,13E-05	0,303264
21,8	0,010076	0,12094	8,76E-05	0,335591
24,5	0,013541	0,140931	0,000118	0,377155
27,4	0,016525	0,15894	0,000144	0,421798

According to the calculated stress and strain, graphs for four configurations were shown in figure 20 a, 20 b, 20 c and 20 d.

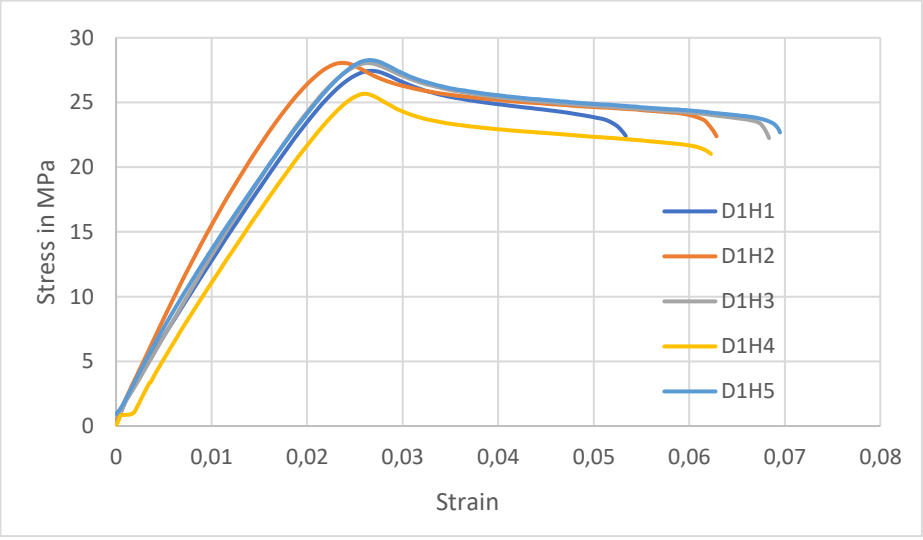

Figure 20 a. Graph for stress vs strain for tensile test -D1H

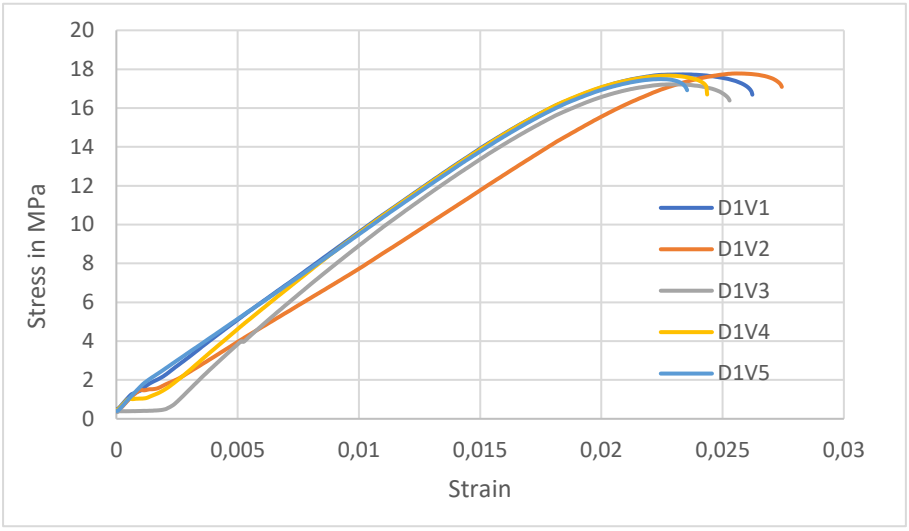

Figure 20 b. Graph for stress vs strain for tensile test -D1V

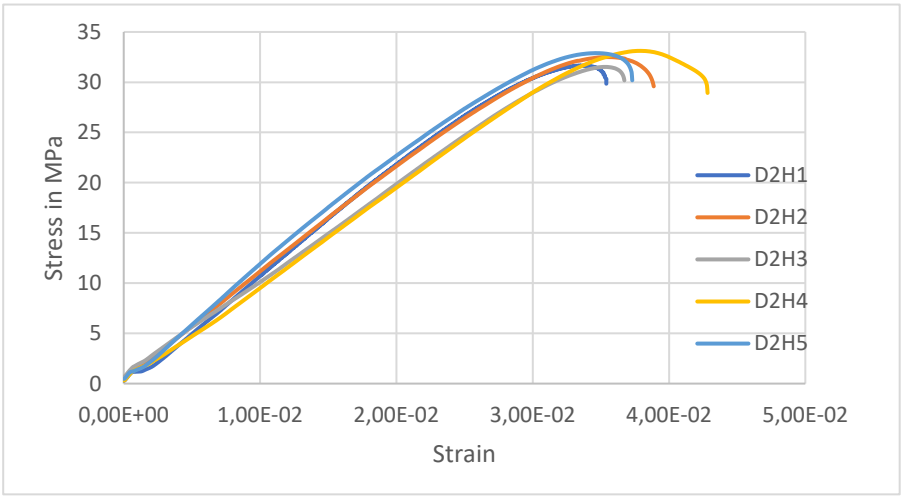

Figure 20 c. Graph for stress vs strain for tensile test -D2H

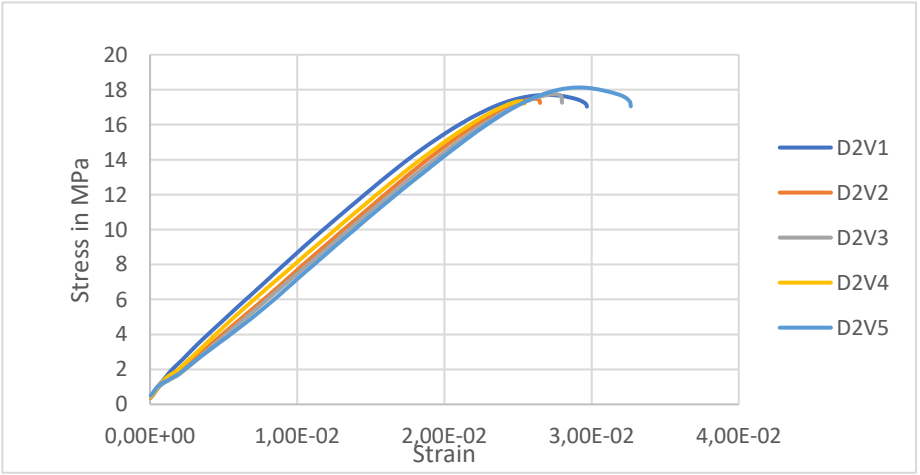

Figure 20 d. Graph for stress vs strain for tensile test -D2V

Calculation of Young modulus and calculation of yield strength using the 0.2% offset method were illustrated in figure 21 a, and figure 21 b.

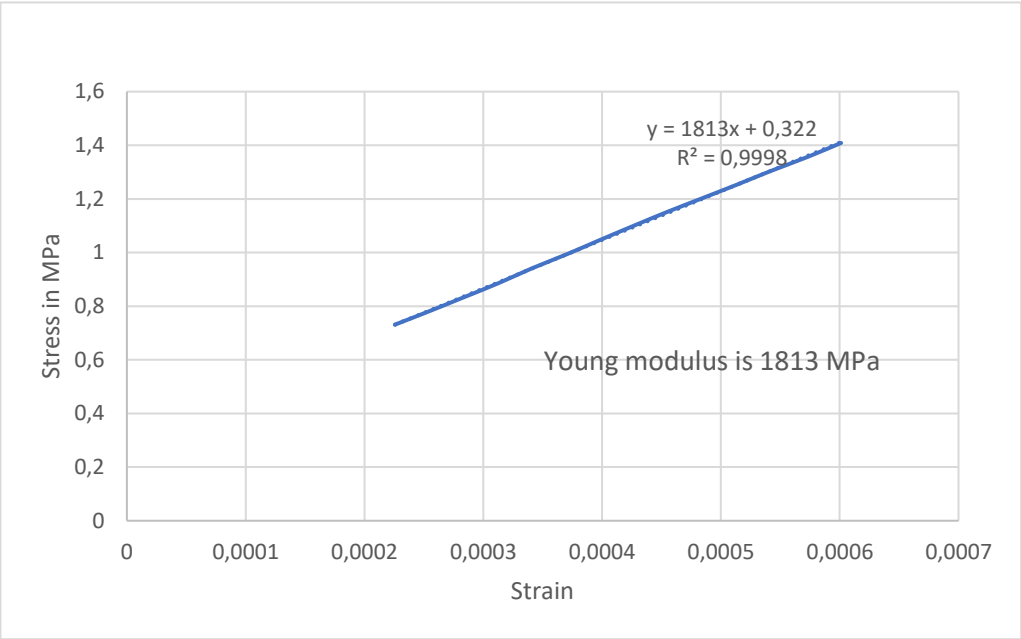

Figure 21 a. Graph for elastic region of the stress vs strain curve for D1H – Specimen 2

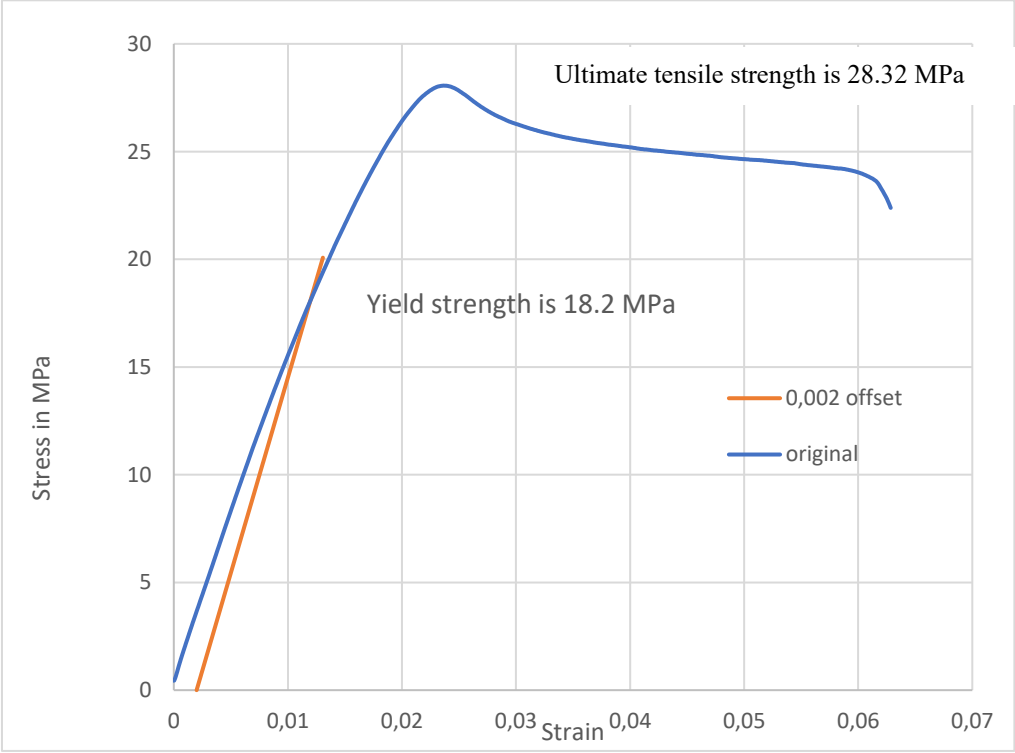

Figure 21 b. Graph for 0,2% offset line for yield strength calculations for D1H – Specimen 2

Similarly, young modulus, yield strength, ultimate tensile strength were obtained from the individual graphs and calculated the mean values. Mean values of them were calculated and tabulated in table 5.

Finally, the average of five values was calculated and tabulated in table 5.

Table 5. Calculated values for tensile test

Calculated Tensile Properties (Average values)				
Tests		Young Modulus (MPa)	Yield Strength (MPa)	Ultimate tensile strength (MPa)
Design 1	Horizontal	1639,8	13,99	27,49
	Vertical	1314,6	6,20	17,58
Design 2	Horizontal	1504,6	7,60	32,33
	Vertical	994,4	7,47	17,68

5.3 Flexural strength

According to the ISO 178 guidelines, the given equations (mentioned under 3.6 chapters) are used to calculate strain, stress and flexural modulus. The flexural strength is the highest value of the calculated stresses.

The calculation of **original stress and strain** is illustrated in table 6.

Table 6. Calculations of original strain and stress using data in CSV file (Design 1 – horizontal flexural specimen 1)

Data from the experiment		Calculations	
		$\varepsilon_f = \frac{6sh}{L^2}$	$\sigma_f = \frac{3FL}{2bh^2}$
F (N) Force	s deflection	ε_f strain	σ_f stress (MPa)
0	0,013461	0,000110422	0
0,2	0,016925	0,000138838	0,052779733
0,4	0,019841	0,000162758	0,105559467
0,6	0,023132	0,000189755	0,158339204
0,8	0,026086001	0,000213987	0,211118933
1	0,029456001	0,000241631	0,263898663
1,2	0,032388002	0,000265683	0,316678408
1,3	0,035293002	0,000289513	0,343068249
1,5	0,038344	0,000314541	0,395847994
1,8	0,041811999	0,000342989	0,475017581
2,1	0,045254	0,000371224	0,554187167

2,3	0,048486002	0,000397737	0,606966912
2,5	0,051973	0,000426341	0,659746657
2,7	0,055162001	0,000452501	0,712526402
2,9	0,058456998	0,00047953	0,765306148
3,1	0,061701	0,000506141	0,81808583
3,2	0,065053999	0,000533646	0,844475734

Calculation of **Flexural modulus**

$\varepsilon_{fi} = 1\ or\ 2\ and\ \ then\ \varepsilon_{f1} = 0.005\ and\ \varepsilon_{f2} = 0.0025$ and

$h = 5.6\ mm, L = 64\ mm \quad and \quad s_i = \frac{\varepsilon_{fi} L^2}{6h}$

$s_1 = 0{,}06952381\ mm$

$s_2 = 0{,}304761905\ mm$

The force was calculated when deflections were S_1 and S_2 from table ….

$F_1 = 3.05\ N$

$F_2 = 20.28\ N$

$\sigma_f = \frac{3FL}{2bh^2}, \qquad \sigma_{f1} = 0.806\ MPa\ and\ \sigma_{f2} = 5{,}351\ MPa$

$E_f = \frac{\sigma_{f2} - \sigma_{f1}}{\varepsilon_{f2} - \varepsilon_{f1}} = 2272.728\ MPa$

Similarly, modulus for all was calculated and tabulated in table 7.

Table 7. Calculated values for Flexural modulus

Flexural Modulus		
Sample		Average in Mpa
Deign 1	Horizontal	2325.412
	Vertical	2024.912
Design 2	Horizontal	2128.464
	Vertical	1928.704

Calculation of **Flexural strength**

The stress vs strain curves for all cases were graphed as shown in figure 22 a, 22 b, 22 c and 22 d.

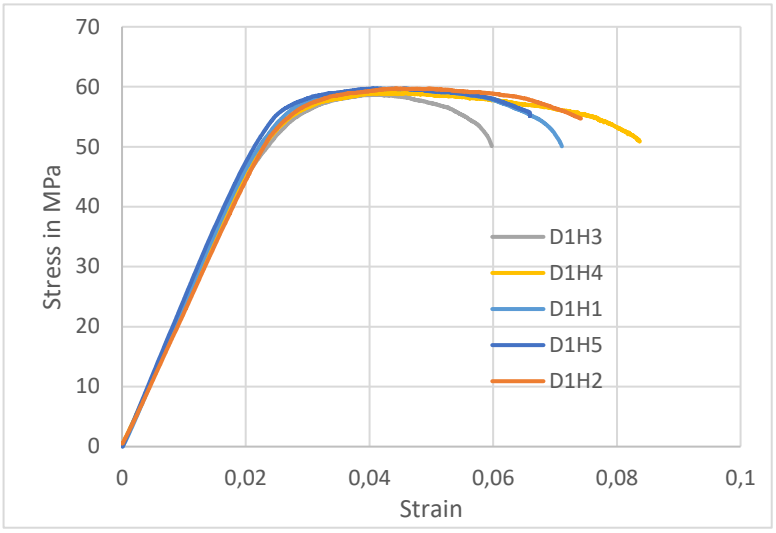

Figure 22 a. Graph for stress vs strain for flexural test for D1H

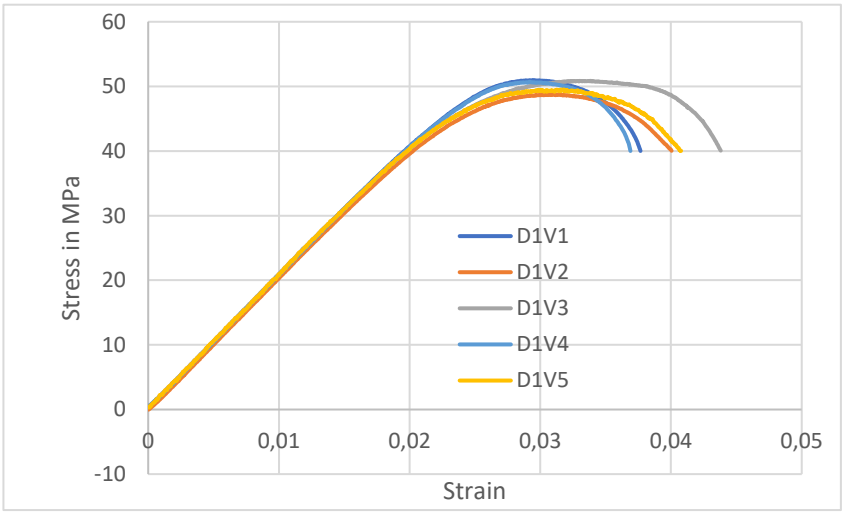

Figure 22 b. Graph for stress vs strain for flexural test for D1V

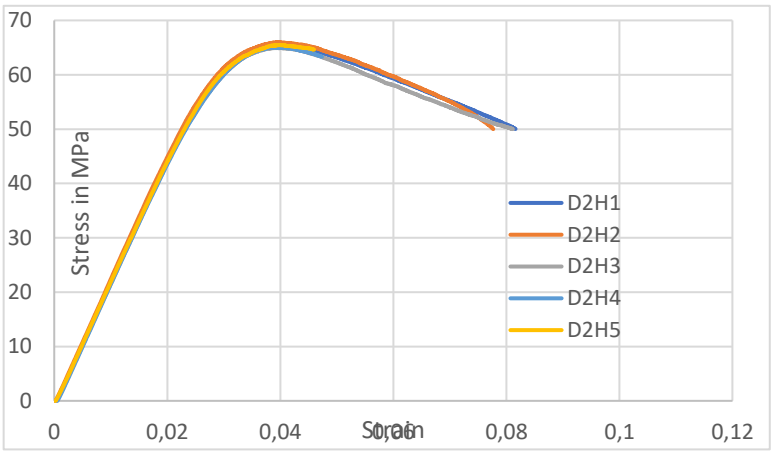

Figure 22 c. Graph for stress vs strain for flexural test for D2H

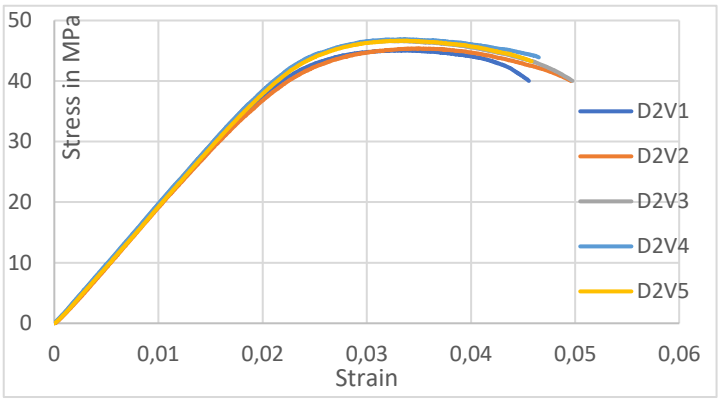

Figure 22 d. Graph for stress vs strain for flexural test for D2V

The maximum value of stress before breaking is represented the Flexural strength. The average values of four configurations are shown in table 8.

Table 8. Calculated values for Flexural strength

Flexural Strength		
Sample		Average in MPa
Deign 1	Horizontal	59,354
	Vertical	50,156
Design 2	Horizontal	65,198
	Vertical	46,114

5.4 Computational Analysis

COMSOL Multiphysics was used to analyse the T1 temperature using other known values such as voltage, current, area, flux, T2 and k. Temperature profiles for each case are shown in figure 23

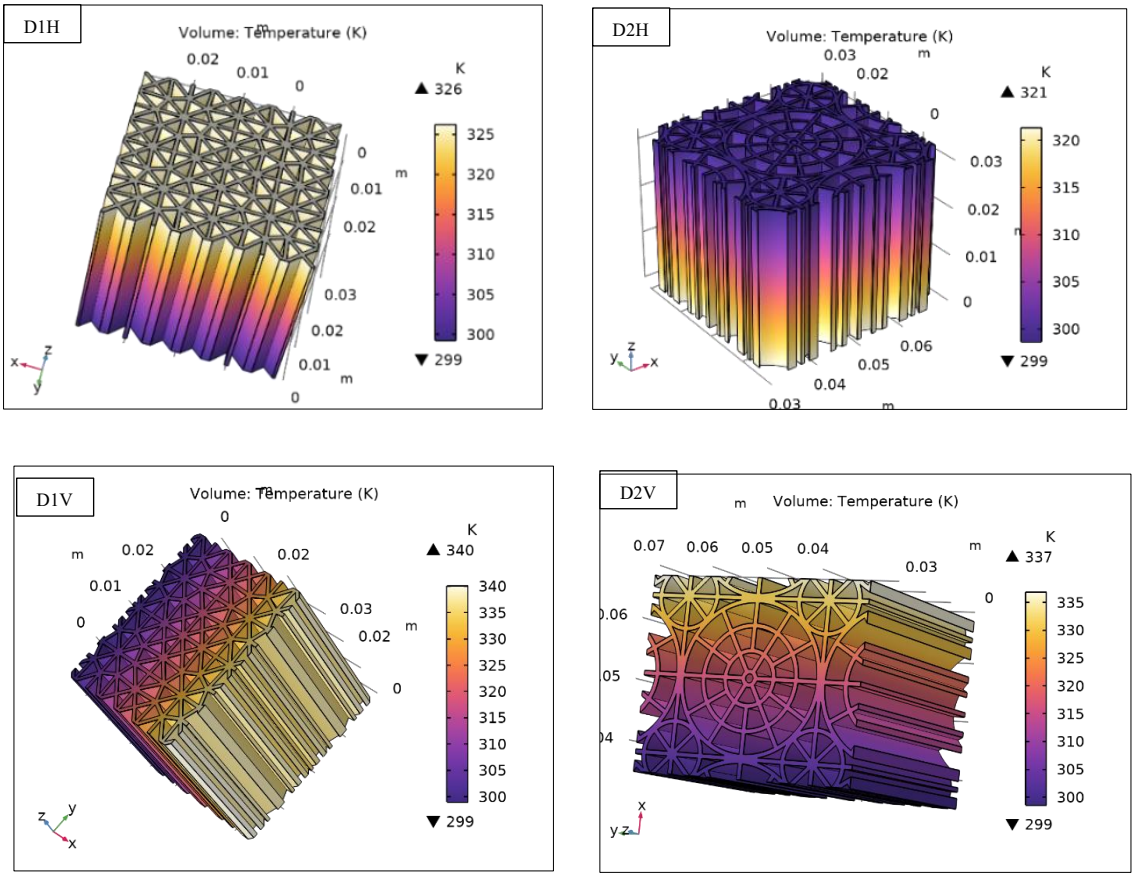

Figure 23. Temperature profiles for all cases by COMSOL

The values which were obtained from COMSOL for T1 are tabulated in table 9.

Table 9. Analysing of T1 from COMSOL

Sample	from COMSOL
	T1 (K)
Design 1 Horizontal	326
Design 1 Vertical	340
Design 2 Horizontal	321
Design 2 Vertical	337

Calculated parameters from all methods are tabulated in table 10.

Table 10. Result obtained from all test methods.

Sample	Tensile test			Flexural test		Thermal test		COMSOL
	Young Modulus (MPa)	Yield Strength (MPa)	Tensile Strength (MPa)	Flexural Modulus (MPa)	Flexural strength (MPa)	Thermal conductivity (W/K.m)	T1 (K)	T1 (K)
Design1 Horizontal (D1H)	1639,80	13,994	27,488	2155,38	58,294	6,211	326,25	326
Design 1 Vertical (D1V)	1314,60	6,204	17,578	2024,912	50,156	6,234	325,85	340
Design 2 Horizontal (D2H)	1504,60	7,60	32,890	2128,464	65,198	7,387	321,35	321
Design 2 Vertical (D2V)	994,40	7,47	17,678	1926,704	46,114	7,657	320,45	337

Comparing the results with previous studies helps to understand the accuracy of the findings. The experimental data from previous studies are tabulated in Table 11.

Table 11. Experimental data from the similar previous studies.

Tensile strength (MPa)	Flexural Strength (MPa)	Thermal conductivity	References
43,36			*73 (Table 1)*
	61,75		*72 (Table 5)* *consider only for honey comb structures*
		1,25 $W/m^2.K$ (u-value)	*74 (Fig 6)* *U valve 1. 25 $W/m^2.K$*

6 Discussion

Considering the tensile properties, horizontal samples have higher young modulus than vertical samples, 1639.8 and 1504.6 MPa for D1H and D2H respectively, while D1V and D2V have 1314.6 and 994.4 MPa. Among the four samples D1H has the highest young modulus. Yield strength shows a mix combination, the highest value for D1H, 13.994 MPa. It is 46 % higher than the next highest value, 7.6 MPa for D2H. The lowest value is for D1H (6.204 MPa). Similarly to the young modulus, tensile strength is higher in horizontal samples than vertical, but D2H has the highest value of 32.8 MPa. It is almost 5.4 MPa increment than D1H. D2V and D1V have very close values, 17.678 and 17.578 MPa. D2H has the best tensile properties over other three samples and the next best one is D1H which has very close figures to D2H.

In flexural, D1H (2155.38 MPa) and D2H (2128.46 MPa) have higher figures in young modulus than D1V (2024.91 MPa) and D2V (1926.70 MPa). However, D1H and D2H have quite equal values. Flexural strength is higher in horizontal components than vertical. Following the same trend in tensile strength, D2H has the highest figure, 65.198 MPa and next highest is D1H, 58.29 MPa. D1V has slightly higher value than D2V, 50.15 MPa and 46.11 MPa respectively. Accordingly, the descending order of the best elements in flexural properties is D2H, D1H, D1V and D2V.

The important property in heat transfer, thermal conductivity of Vertical samples is bigger than the horizontal samples. D2H and D2V both exceed the thermal conductivity value of design 1. The value of vertical components is 7.65 W/K.m (D2V), 7.38 W/K.m (D2V) and the horizontal are 6.234 W/K.m (D2V) and 6.21 W/K.m (D1H). Among the 4 samples D2V is the best in heat transfer and D1H has the least value.

Altogether, in mechanical properties (tensile and flexural), D2H is the strongest element and the second strongest element is D1H while D2V is the least strong element. Considering all 3 category, D2H sample has the best mechanical properties while D2V has the best thermal conductivity.

The heated surface temperature (T1) which was obtained from the experiment and COMSOL show a similarity in horizontal direction but a considerable deviation in vertical direction. The difference between experimental and COMSOL values are less than 0,5 K in both design while COMSOL value for D1V is 340 K which is 14.15K higher than the experimental value. For D2V the difference is 16.55 K.

However, the previous experiments values are deviating for tensile, but there is a similarity with flexural. The previous values are 43.36 MPa, but the highest value which obtained from this thesis is 32.89 for D2H, recording 25% reduction in tensile strength. The flexural values lay in same range from 58 - 65 MPa for horizontal and the previous value is around 61 MPa. The vertical values show a considerable reduction of 11 - 15 MPa [72, 73].

In thermally, available study gives a U value of 1,25 W/m^2. K and it is very low value, comparing with the value of this thesis [74]. The U value of this study for the D2V is 194 W/m2. K.

According to the above description, it is revealed that the Design 1- horizontal is the most favourable for mechanical applications, with high stiffness and strength among the four configurations. Design 2 – horizontal is strong in mechanical performance, especially in flexural strength.

The vertically printed samples are good in thermal than horizontal components and they are good for thermal management purposes. For insulation purposes, Design 1 – is the most suitable choice among the four configurations.

7 Conclusions

This study investigated the impact the different geometries and orientations fabricated using Hyper PLA filament through the FFF process, on thermal and mechanical properties. To achieve this target several steps were followed. First referring the existing research to find the research gap, the theory behind, to get familiar with available experimental methods and the equipment etc. It was somewhat a challenged to design an own geometry design, because the all-basic shapes triangle, square, rectangle etc., were used for different types of studies. Two different geometries with triangle and circles were designed with SolidWorks. Two different directions were considered and named as Design 1- horizontal, Design 1 – vertical, Design 2- horizontal and Design 2 – vertical. All configurations were subjected to thermal, tensile, flexural with the test specimens printed with Fused filament fabrication with Hyper PLA material. Finally, a computational thermal analysis was carried out by COMSOL Multiphysics software. Considering all results obtained from thermal tests, mechanical tests and COMSOL, discussion was made.

The best element for mechanical purposes is DH2, and next most suitable element is D1H. It proofs that, the element can bear more tensile and flexural stress in perpendicular direction to the design due to undisturbed fibres. Parallel direction to the design, the fibres discontinue according to the pattern. But heat dissipation is good in the vertical direction than horizontal direction, because printing layer can transfer heat better than horizontal direction.

The both vertical and horizontal components of Design 2 have high conductivity than both components of design 1. Then, geometry affects the thermal properties of the object. Further, the conductivity values which obtained from the experiment is higher than the available thermal insulation materials which lays lesser than the 0.1 W/K.m [76].

The COMSOL shows the difference of T1 temperature in vertical direction of both designs. Considering the specimen for heat trans test, the specimen in horizontal direction has the flat surfaces which were contacted with heat pad. Therefore, heat loss could be neglected. But in vertical direction, approximately half of the area was touched with the hot pad and the heat dissipation would not be happening in full area of the specimen. Hence, the actual value could be lesser than the computational value.

According to the mechanical and thermal values, it can be recommended, the tested samples are good for non-load bearing structural application and the moderate heat transfer applications.

The future studies may be invested on a wider variety of internal geometries with different size of voids, to find sustainable solution insulation application.

References

1. Kadi, Y., Ammar Korichi, & Maalouf, C. (2023). Improving building energy efficiency and thermal comfort with natural fibre insulation. *Proceedings of the Institution of Civil*

Engineers - Engineering Sustainability, *177*(4), 230–241. https://doi.org/10.1680/jensu.21.00003

2. Ye, X., Lu, J., Gong, Q., Zhang, T., Wang, Y., & Fukuda, H. (2024). Measuring effects of insulation renewal on heating energy and indoor thermal environment in urban residence of hot-summer/cold-winter region, China. *Case Studies in Thermal Engineering*, *61*, 104982. https://doi.org/10.1016/j.csite.2024.104982
3. IEA. (2023, July 11). *Buildings - Energy System*. IEA. https://www.iea.org/energy-system/buildings
4. *Where to start? Energy use in buildings Buildings IEA #energyefficientworld Buildings energy efficiency sessions in partnership with: INDO-SWISS BUILDING ENERGY EFFICIENCY PROJECT*. (n.d.). https://iea.blob.core.windows.net/assets/imports/events/613/Building
5. *Fiberglass Insulation*. (n.d.). Design Life-Cycle. https://www.designlife-cycle.com/fiberglass-insulation
6. Tettey, U. Y. A., Dodoo, A., & Gustavsson, L. (2014). Effects of different insulation materials on primary energy and CO2 emission of a multi-storey residential building. *Energy and Buildings*, *82*, 369–377. https://doi.org/10.1016/j.enbuild.2014.07.009
7. Associates, F. (2009). *ENERGY AND GREENHOUSE GAS SAVINGS FOR EPS FOAM INSULATION APPLIED TO EXTERIOR WALLS OF SINGLE FAMILY RESIDENTIAL HOUSING IN THE U.S. AND CANADA Final Revised Report Prepared for The EPS Molders Association Crofton, MD*. https://www.airfoam.com/rigid-insulation/Life-Cycle-Analysis-EPS-Expanded-Polystyrene-Franklin-2009.pdf
8. Ahart, M. (2019, June 3). *Types of 3D Printing Explained*. Www.protolabs.com. https://www.protolabs.com/resources/blog/types-of-3d-printing/
9. *CNC Machining, Sheet Metal, Injection Moulding, 3D Printing and more | Geomiq*. (2021). Geomiq.com. https://geomiq.com/3d-printing-guide
10. Ahart, M. (2019, June 3). *Types of 3D Printing Explained*. Www.protolabs.com. https://www.protolabs.com/resources/blog/types-of-3d-printing/
11. *3D Prima - 3D-Printers and filaments*. (2017). 3dprima.com. https://www.3dprima.com/
12. Fico, D., Rizzo, D., Casciaro, R., & Esposito Corcione, C. (2022). A Review of Polymer-Based Materials for Fused Filament Fabrication (FFF): Focus on Sustainability and Recycled Materials. *Polymers*, *14*(3), 465. https://doi.org/10.3390/polym14030465
13. Khan, M. (2023, April 12). *The Ultimate Guide to Materials Used in 3D Printing*. Wevolver. https://www.wevolver.com/article/20240408-the-ultimate-guide-to-materials-used-in-3d-printing
14. Technologies, S. (2022, March 28). *Fused Deposition Modeling Advantages and Disadvantages*. SyBridge Technologies. https://sybridge.com/fused-deposition-modeling-advantages-and-disadvantages/
15. Altıparmak, S. C., Yardley, V. A., Shi, Z., & Lin, J. (2022). Extrusion-based additive manufacturing technologies: State of the art and future perspectives. *Journal of Manufacturing Processes*, *83*, 607–636. https://doi.org/10.1016/j.jmapro.2022.09.032
16. afalcon. (2024, February 13). *Study of the impact of 3D printing parameters on the mechanical properties of FFF samples - BCN3D Technologies*. BCN3D Technologies. https://www.bcn3d.com/study-of-the-impact-of-3d-printing-parameters-on-the-mechanical-properties-of-fff-samples/
17. *Introduction to FFF 3D printing technology & its most important parameters*. (2018, July 18). BCN3D Technologies. https://www.bcn3d.com/introduction-fff-technology-3d-printing-important-parameters/ *Introduction to FFF 3D printing technology & its most important parameters*. (2018, July 18). BCN3D Technologies. https://www.bcn3d.com/introduction-fff-technology-3d-printing-important-parameters/

Introduction to FFF 3D printing technology & its most important parameters. (2018, July 18). BCN3D Technologies. https://www.bcn3d.com/introduction-fff-technology-3d-printing-important-parameters/

18. *Cura Infill Patterns and Settings – MeaD MaDe*. (2024). Itsmeadmade.com. https://itsmeadmade.com/cura-infill-patterns-and-settings/
19. O'Neill, B. (2024, April 13). *Cura Infill Patterns: What They Are and When to Use Them*. Www.wevolver.com. https://www.wevolver.com/article/cura-infill-patterns
20. Kharat, V. J., Singh, P., Sharath Raju, G., Kumar Yadav, D., Satyanarayana.Gupta, M., Arun, V., Hussein Majeed, A., & Singh, N. (2023). Additive manufacturing (3D printing): A review of materials, methods, applications and challenges. *Materials Today: Proceedings*. https://doi.org/10.1016/j.matpr.2023.11.033
21. Srinivas, K. (n.d.). *A New Approach to Product Development & Rapid Prototyping*. Retrieved November 8, 2024, from https://advanses.com/wp-content/uploads/2021/05/mechanical-testing-3d-printed-small-size.pdf
22. Michał Góra, Bańkosz, M., & Bożena Tyliszczak. (2024). Use of Innovative Methods to Produce Highly Insulating Walls Using 3D-Printing Technology. *Materials*, *17*(16), 3990–3990. https://doi.org/10.3390/ma17163990
23. Fico, D., Rizzo, D., Casciaro, R., & Esposito Corcione, C. (2022). A Review of Polymer-Based Materials for Fused Filament Fabrication (FFF): Focus on Sustainability and Recycled Materials. *Polymers*, *14*(3), 465. https://doi.org/10.3390/polym14030465
24. Sélo, R. R. J., Catchpole-Smith, S., Maskery, I., Ashcroft, I., & Tuck, C. (2020). On the thermal conductivity of AlSi10Mg and lattice structures made by laser powder bed fusion. *Additive Manufacturing*, *34*, 101214. https://doi.org/10.1016/j.addma.2020.101214
25. Zhou, Y., Shen, S., Liu, T., Li, P., & Duan, F. (2023). *Effective Heat Conduction Evaluation of Lattice Structures from Selective Laser Melting Printing*. https://doi.org/10.2139/ssrn.4458771
26. Kamata, M., Hayashi, K., Watanabe, N., Nakazawa, K., Tsuru, T., Akizuki, Y., & Nagano, H. (2024). Thermal performance of ammonia-based thin flat loop heat pipe fabricated by additive manufacturing. *International Journal of Heat and Mass Transfer*, *236*, 126382. https://doi.org/10.1016/j.ijheatmasstransfer.2024.126382
27. Orkhan Huseynov, Seymur Hasanov, & Ismail Fidan. (2023). Influence of the matrix material on the thermal properties of the short carbon fiber reinforced polymer composites manufactured by material extrusion. *Journal of Manufacturing Processes*, *92*, 521–533. https://doi.org/10.1016/j.jmapro.2023.02.055
28. Panda, B., Leite, M., Biswal, B. B., Niu, X., & Garg, A. (2018). Experimental and numerical modelling of mechanical properties of 3D printed honeycomb structures. *Measurement*, *116*, 495–506. https://doi.org/10.1016/j.measurement.2017.11.037
29. Jiang, H., Jia, R., Aiyiti, W., Aihemaiti, P., & Kasimu, A. (2023). Infill strategies for 3D-printed CF-PEEK/HA-PEEK honeycomb core-shell composite structures. *Journal of Manufacturing Processes*, *92*, 338–349. https://doi.org/10.1016/j.jmapro.2023.02.058
30. Alqahtani, S., Ali, H. M., Farukh, F., Silberschmidt, V. V., & Kandan, K. (2021). Thermal performance of additively manufactured polymer lattices. *Journal of Building Engineering*, *39*, 102243. https://doi.org/10.1016/j.jobe.2021.102243
31. Alqahtani, S., Alqahtani, T., Ali, H. M., Farukh Farukh, & Karthikeyan Kandan. (2024). The effect of lattice topology on the thermal and mechanical performance of additively manufactured polymer lattices. *Results in Engineering*, 101905–101905. https://doi.org/10.1016/j.rineng.2024.101905
32. Taleb, O., Jutkofsky, M., Measel, R., Blatt, M. P., Hmeidat, N., Barnett, P., Koerner, H., & jr, H. (2024). Thermal conductivity of 3D-printed block-copolymer-inspired

structures. *International Journal of Heat and Mass Transfer*, *235*, 126186–126186. https://doi.org/10.1016/j.ijheatmasstransfer.2024.126186
33. de Rubeis, T., Ciccozzi, A., Giusti, L., & Ambrosini, D. (2022). The 3D Printing Potential for Heat Flow Optimization: Influence of Block Geometries on Heat Transfer Processes. *Sustainability*, *14*(23), 15830. https://doi.org/10.3390/su142315830
34. de Rubeis, T. (2022). 3D-Printed Blocks: Thermal Performance Analysis and Opportunities for Insulating Materials. *Sustainability*, *14*(3), 1077. https://doi.org/10.3390/su14031077
35. de Rubeis, T., Ciccozzi, A., Pasqualoni, G., Paoletti, D., & Ambrosini, D. (2023). On the Use of Waste Materials for Thermal Improvement of 3D-Printed Block—An Experimental Comparison. *Buildings*, *13*(5), 1136. https://doi.org/10.3390/buildings13051136
36. Bahar, A., El, A., Ferhat Benmahiddine, Sofiane Belhabib, Rafik Belarbi, & Sofiane Guessasma. (2023). The Thermal and Mechanical Behaviour of Wood-PLA Composites Processed by Additive Manufacturing for Building Insulation. *Polymers*, *15*(14), 3056–3056. https://doi.org/10.3390/polym15143056
37. Pei, Y., Shen, Z., Zhou, J., & Yang, B. (2024). Experimental and theoretical thermal performance analysis of additively manufactured polymer vacuum insulation panels. *Applied Thermal Engineering*, 123957–123957. https://doi.org/10.1016/j.applthermaleng.2024.123957
38. Anwajler, B., Jerzy Szołomicki, Paweł Noszczyk, & Michał Baryś. (2024). The Potential of 3D Printing in Thermal Insulating Composite Materials—Experimental Determination of the Impact of the Geometry on Thermal Resistance. *Materials*, *17*(5), 1202–1202. https://doi.org/10.3390/ma17051202
39. Li, S., Xin, J., & Chen, R. (2024). Achieving high strength and low thermal conductivity: Additive manufacturing of mullite lightweight refractory. *Ceramics International*, *50*(16), 27880–27888. https://doi.org/10.1016/j.ceramint.2024.05.084
40. Chung, S.-Y., Stephan, D., Elrahman, M. A., & Han, T.-S. (2016). Effects of anisotropic voids on thermal properties of insulating media investigated using 3D printed samples. *Construction and Building Materials*, *111*, 529–542. https://doi.org/10.1016/j.conbuildmat.2016.02.165
41. Forés-Garriga, A., Gómez-Gras, G., & Pérez, M. A. (2022). Mechanical performance of additively manufactured lightweight cellular solids: Influence of cell pattern and relative density on the printing time and compression behavior. *Materials & Design*, *215*, 110474. https://doi.org/10.1016/j.matdes.2022.110474
42. PTC. (2024). *What is CAD?| Computer-Aided Design | PTC*. Www.ptc.com. https://www.ptc.com/en/technologies/cad
43. BasuMallick, C. (2022, September 27). *What is CAD (Computer Aided Design)? Definition, Types, and Applications*. Spiceworks. https://www.spiceworks.com/tech/devops/articles/what-is-cad/
44. McClements, D. (2024, March 15). *Computer-Aided Design (CAD) Modeling: Definition, Types, and Examples*. Www.xometry.com. https://www.xometry.com/resources/3d-printing/cad-modeling/
45. *19 Types of CAD Software: Definition, Lists and Benefits*. (2025). Indeed Career Guide. https://sg.indeed.com/career-advice/career-development/cad-software
46. *SOLIDWORKS*. (2025, March 31). TECHNIA. https://www.technia.com/en/engineering/software/solidworks/
47. Solidworks. (2017, November 27). *SOLIDWORKS 3D CAD*. SOLIDWORKS. https://www.solidworks.com/product/solidworks-3d-cad
48. Symestic. (2024, April 30). *Computer-Aided Engineering (CAE)*. Symestic.com; symestic GmbH. https://www.symestic.com/en-us/what-is/cae
49. Siemens. (n.d.). *Computer-aided engineering (CAE)*. Siemens Digital Industries Software. https://www.sw.siemens.com/en-US/technology/computer-aided-engineering-cae/

50. *Computer-Aided Engineering (CAE) Software*. (2025, May 26). Saasworthy.com. https://www.saasworthy.com/list/computer-aided-engineering-cae-software
51. COMSOL. (2020). *COMSOL Multiphysics®*. COMSOL Multiphysics®. https://www.comsol.com/comsol-multiphysics
52. COMSOL. (2019). *COMSOL Multiphysics® Modeling Software*. Comsol.com. https://www.comsol.com/
53. *About COMSOL - Multiphysics Simulation Software Provider*. (n.d.). Www.comsol.com. https://www.comsol.com/company
54. McClements, D. (2022, May 4). *Everything You Need to Know About 3D Printing*. Www.xometry.com. https://www.xometry.com/resources/3d-printing/3d-printing-guide/
55. *3D Printing Polymers: Types, Materials & Processing Methods*. (2020). Specialchem.com. https://omnexus.specialchem.com/selection-guide/3d-printing-polymers
56. *What is 3D Printing? A complete guide on processes, applications, pros, and cons*. (2021). Geomiq.com. https://geomiq.com/3d-printing-guide/
57. Loughborough University. (2010). *The 7 categories of Additive Manufacturing | Additive Manufacturing Research Group | Loughborough University*. Lboro.ac.uk. https://www.lboro.ac.uk/research/amrg/about/the7categoriesofadditivemanufacturing
58. *Thermal Management Theory--Thermal Conductivity Theories and Specific Thermal Management Methods for Thermal Design ⎪Taiyo Wire Cloth has a wide core technology and design development capability and provides solutions to customers.* (2024). Taiyo Wire Cloth . https://www.twc-net.com/blog/uncategorized/a38
59. C-Therm C-Therm. (2022, May 30). *What is Thermal Conductivity? How is it Measured? – TAL*. C-Therm Technologies Ltd. https://ctherm.com/resources/newsroom/blog/what-is-thermal-conductivity
60. Thermtest Instruments. (2017). *What Is Thermal Conductivity? an Overview*. Thermtest Inc. https://thermtest.com/what-is-thermal-conductivity
61. Kat De Naoum. (2023, March 23). *Tensile Strength: Definition, Importance, Types, and Examples*. Www.xometry.com. https://www.xometry.com/resources/3d-printing/tensile-strength/
62. Omnexus. (2025). *Tensile Strength - Definition, Units, Formula & Test Methods*. Omnexus.specialchem.com. https://omnexus.specialchem.com/polymer-property/strength-at-break-tensile
63. Ahmed, R. (2023, July 27). *What is Ultimate Tensile Strength?* Metal Supermarkets. https://www.metalsupermarkets.com/what-is-ultimate-tensile-strength/
64. Anup KumarH S. (2022, July 1). *The 0.2% Offset Method for Yield Stress*. Skill-Lync. https://skill-lync.com/blogs/the-02-percent-offset-method-for-yield-stress
65. Langnau, L. (2019, December 18). *What is flexural strength? - Engineering.com*. Engineering.com. https://www.engineering.com/what-is-flexural-strength/
66. *What Is Flexural Strength - company news - News*. (n.d.). Www.hlc-Metalparts.com. https://www.hlc-metalparts.com/news/what-is-flexural-strength-78043665.html
67. Egan, M. (2023, December 21). *Understanding Flexural Strength: Guide to Flexural Strength in Materials*. Atlas Fibre. https://www.atlasfibre.com/understanding-flexural-strength-guide-to-flexural-strength-in-materials/
68. Anwajler, B., Jerzy Szołomicki, Paweł Noszczyk, & Michał Baryś. (2024). The Potential of 3D Printing in Thermal Insulating Composite Materials—Experimental Determination of the Impact of the Geometry on Thermal Resistance. *Materials*, *17*(5), 1202–1202. https://doi.org/10.3390/ma17051202
69. Alqahtani, S., Alqahtani, T., Ali, H. M., Farukh Farukh, & Karthikeyan Kandan. (2024). The effect of lattice topology on the thermal and mechanical performance of additively manufactured polymer lattices. *Results in Engineering*, 101905–101905. https://doi.org/10.1016/j.rineng.2024.101905

70. *Machine*. (n.d.). Testometric. https://www.testometric.co.uk/product/machine/x350/x350-machine/

71. Travieso-Rodriguez, J. A., Jerez-Mesa, R., Llumà, J., Traver-Ramos, O., Gomez-Gras, G., & Roa Rovira, J. J. (2019). Mechanical Properties of 3D-Printing Polylactic Acid Parts subjected to Bending Stress and Fatigue Testing. *Materials*, *12*(23), 3859. https://doi.org/10.3390/ma12233859

72. Kahya, Ç., Tunçel, O., Çavuşoğlu, O., & Tüfekci, K. (2025). Thermal annealing optimization for improved mechanical performance of PLA parts produced via 3D printing. *Polymer Testing*, *144*, 108735. https://doi.org/10.1016/j.polymertesting.2025.108735

73. Kechagias, J. D., & Zaoutsos, S. P. (2024). An assessment of PLA/wood with PLA core sandwich multilayer component tensile strength under different 3D printing conditions. *Journal of Manufacturing Processes*, *131*, 1240–1249. https://doi.org/10.1016/j.jmapro.2024.09.098

74. Alqahtani, S., Ali, H. M., Farukh, F., Silberschmidt, V. V., & Kandan, K. (2021). Thermal performance of additively manufactured polymer lattices. *Journal of Building Engineering*, *39*, 102243. https://doi.org/10.1016/j.jobe.2021.102243

75. *Hyper-PLA Filament Technical Data Sheet Version 1.0 i*. (n.d.). Retrieved May 27, 2025, from https://download.bastelgarage.ch/Produkte/TDS_Hyper%20PLA(EN).pdf

76. Asdrubali, F., D'Alessandro, F., & Schiavoni, S. (2015). A review of unconventional sustainable building insulation materials. *Sustainable Materials and Technologies*, *4*(4), 1–17. https://doi.org/10.1016/j.susmat.2015.05.002